



**NAVAL
POSTGRADUATE
SCHOOL**

MONTEREY, CALIFORNIA

THESIS

**EXTRACTION OF A WEAK CO-CHANNEL
INTERFERING COMMUNICATION SIGNAL USING
ADAPTIVE FILTERING**

by

Woei Chieh Lee

March 2015

Thesis Advisor:

Monique P. Fargues

Thesis Co-Advisor:

Roberto Cristi

Approved for public release; distribution is unlimited

THIS PAGE INTENTIONALLY LEFT BLANK

REPORT DOCUMENTATION PAGE			Form Approved OMB No. 0704-0188	
Public reporting burden for this collection of information is estimated to average 1 hour per response, including the time for reviewing instruction, searching existing data sources, gathering and maintaining the data needed, and completing and reviewing the collection of information. Send comments regarding this burden estimate or any other aspect of this collection of information, including suggestions for reducing this burden to Washington headquarters Services, Directorate for Information Operations and Reports, 1215 Jefferson Davis Highway, Suite 1204, Arlington, VA 22202-4302, and to the Office of Management and Budget, Paperwork Reduction Project (0704-0188) Washington DC 20503.				
1. AGENCY USE ONLY (Leave Blank)	2. REPORT DATE 03-27-2015	3. REPORT TYPE AND DATES COVERED Master's Thesis 05-28-2014 to 03-27-2015		
4. TITLE AND SUBTITLE EXTRACTION OF A WEAK CO-CHANNEL INTERFERING COMMUNICATION SIGNAL USING ADAPTIVE FILTERING			5. FUNDING NUMBERS	
6. AUTHOR(S) Woei Chieh Lee				
7. PERFORMING ORGANIZATION NAME(S) AND ADDRESS(ES) Naval Postgraduate School Monterey, CA 93943			8. PERFORMING ORGANIZATION REPORT NUMBER	
9. SPONSORING / MONITORING AGENCY NAME(S) AND ADDRESS(ES) N/A			10. SPONSORING / MONITORING AGENCY REPORT NUMBER	
11. SUPPLEMENTARY NOTES The views expressed in this document are those of the author and do not reflect the official policy or position of the Department of Defense or the U.S. Government. IRB Protocol Number: N/A.				
12a. DISTRIBUTION / AVAILABILITY STATEMENT Approved for public release; distribution is unlimited			12b. DISTRIBUTION CODE	
13. ABSTRACT (maximum 200 words) Conventional separation techniques such as filters cannot be used in a scenario where a weak signal is embedded within a stronger signal in the same frequency band. An adaptive filter approach to recover a weak narrowband communication signal embedded in a strong wideband broadcast signal and additive noise is investigated by taking advantage of the known characteristics of the broadcast signal standard. The weak signal considered is a four-quadrature amplitude modulation (QAM) communication signal, and the stronger signal is a Digital Terrestrial Multimedia Broadcasting (DTMB) signal, which is the digital television standard for People's Republic of China. The results show that, while the extraction of the weak signal is possible, the characteristics of the transmission channel must be very accurately estimated for the scheme to achieve a reasonable error rate.				
14. SUBJECT TERMS Adaptive filter, signal separation			15. NUMBER OF PAGES 71	
			16. PRICE CODE	
17. SECURITY CLASSIFICATION OF REPORT Unclassified	18. SECURITY CLASSIFICATION OF THIS PAGE Unclassified	19. SECURITY CLASSIFICATION OF ABSTRACT Unclassified	20. LIMITATION OF ABSTRACT UU	

THIS PAGE INTENTIONALLY LEFT BLANK

Approved for public release; distribution is unlimited

**EXTRACTION OF A WEAK CO-CHANNEL INTERFERING
COMMUNICATION SIGNAL USING ADAPTIVE FILTERING**

Woei Chieh Lee
Military Expert 5, Republic of Singapore Navy
B. Eng, National University of Singapore, 2002

Submitted in partial fulfillment of the
requirements for the degree of

MASTER OF SCIENCE IN ELECTRICAL ENGINEERING

from the

**NAVAL POSTGRADUATE SCHOOL
March 2015**

Author: Woei Chieh Lee

Approved by: Monique P. Fargues
Thesis Co-Advisor

Roberto Cristi
Thesis Co-Advisor

R. Clark Robertson
Chair, Department of Electrical and Computer Engineering

THIS PAGE INTENTIONALLY LEFT BLANK

ABSTRACT

Conventional separation techniques such as filters cannot be used in a scenario where a weak signal is embedded within a stronger signal in the same frequency band. An adaptive filter approach to recover a weak narrowband communication signal embedded in a strong wideband broadcast signal and additive noise is investigated by taking advantage of the known characteristics of the broadcast signal standard. The weak signal considered is a four-quadrature amplitude modulation (QAM) communication signal, and the stronger signal is a Digital Terrestrial Multimedia Broadcasting (DTMB) signal, which is the digital television standard for People's Republic of China. The results show that, while the extraction of the weak signal is possible, the characteristics of the transmission channel must be very accurately estimated for the scheme to achieve a reasonable error rate.

THIS PAGE INTENTIONALLY LEFT BLANK

Table of Contents

1	Introduction	1
1.1	Motivation	1
1.2	Past Work	1
1.3	Approach	2
1.4	Thesis Organization	3
2	Theoretical Background	5
2.1	Adaptive Noise Cancellation	5
2.2	Structure of DTMB Signal	6
2.3	Channel Estimation for DTMB Signal	6
3	Methodology	9
3.1	Schematic of Overall Implementation	9
3.2	Preprocessing for Adaptive Noise Cancellation	9
3.3	Adaptive Noise Cancellation	10
3.4	Simulink Implementation	11
3.5	Simulations	12
4	Results and Discussions	15
4.1	Need for Multiple Trials	15
4.2	Effect of Number of Coefficients in Channel Estimate	16
4.3	Effect of Error in Channel Coefficients	17
5	Conclusions	25
5.1	Summary	25
5.2	Recommendations for Future Work	25
	Appendix A Simulink Models	27

Appendix B	MATLAB Code	31
B.1	Code to Run Simulation	31
B.2	Code for Initialization	34
B.3	Code to Enable Parallel Computing	37
Appendix C	Supplementary Plots	43
List of References		45
Initial Distribution List		49

List of Figures

Figure 1.1	Plot showing a weak co-channel communication signal embedded within a strong television broadcast signal.	2
Figure 1.2	Areas of the world where ATSC, DVB-T and DTMB are used.	3
Figure 2.1	Typical structure of a basic adaptive noise canceler.	5
Figure 2.2	Structure of the DTMB signal frame.	6
Figure 2.3	Frame headers of various length.	7
Figure 3.1	Schematic of overall setup.	9
Figure 3.2	Preprocessor for adaptive noise cancellation.	10
Figure 3.3	Adaptive noise canceler block.	11
Figure 3.4	Simulink implementation of the preprocessor.	12
Figure 4.1	Plot of SER against INR with 42 000 symbols transmitted per INR.	17
Figure 4.2	Plot of SER against INR with 42 000 symbols transmitted per INR over 100 trials.	19
Figure 4.3	Plot of mean SER against INR with different number of coefficients k in the estimated CIR averaged over 100 trials.	20
Figure 4.4	Plot of mean SER against INR for different number of coefficients k in the estimated CIR averaged over 100 trials with error bars.	21
Figure 4.5	Typical plot of estimated CIR $\hat{h}(n)$	22
Figure 4.6	Plot of mean SER against INR for different errors in estimated channel coefficients averaged over 100 trials.	22
Figure 4.7	Plot of mean SER against INR for different errors in estimated channel coefficient values averaged over 100 trials with error bars.	23

Figure A.1	Overall Simulink model.	27
Figure A.2	Simulink model for communication signal modulator.	28
Figure A.3	Simulink model for DTMB modulator.	28
Figure A.4	Simulink model for transmission channel.	28
Figure A.5	Simulink model for preprocessor and adaptive noise canceler. . .	29
Figure A.6	Simulink model for the DTMB demodulator and the channel estimator within the DTMB demodulator.	30
Figure A.7	Simulink model for the first communication signal demodulator. .	30
Figure A.8	Simulink model for the second communication signal demodulator.	30
Figure C.1	Plot showing distribution of the 100 observations of SER for each INR value for different number of coefficients k in $\hat{h}(n)$	43
Figure C.2	Plot showing distribution of the 100 observations of SER for each INR value for different percentages of error in the channel coefficients.	44

List of Tables

Table 3.1	Simulation parameters for television broadcast signal.	13
Table 3.2	Simulation parameters for the communication signal.	13
Table 3.3	Characteristics for the multipath channel.	14
Table 3.4	Characteristics for the NLMS adaptive filter.	14

THIS PAGE INTENTIONALLY LEFT BLANK

List of Acronyms and Abbreviations

ATSC	Advanced Television Systems Committee
AWGN	additive white Gaussian noise
CIR	channel impulse response
DTMB	Digital Terrestrial Multimedia Broadcasting
DVB-T	Digital Video Broadcasting-Terrestrial
FFT	fast Fourier transform
INR	interference-to-noise ratio
NLMS	normalized-least-mean-square
OFDM	orthogonal frequency-division multiplexing
SER	symbol error ratio
SIR	signal-to-interference ratio
SNR	signal-to-noise ratio
QAM	quadrature amplitude modulation

THIS PAGE INTENTIONALLY LEFT BLANK

Executive Summary

Consider a scenario where a weak signal such as a communication signal is embedded within a strong signal such as a television broadcast signal. Both signals overlap the same frequency band and cannot be separated by filtering in the frequency domain. We investigate an adaptive filter approach to recover the weak narrowband communication signal embedded in the strong wideband television broadcast signal and additive white Gaussian noise (AWGN) by taking advantage of the known characteristics of the television broadcast standard. If successful, the technique could be developed to allow the military to create a covert communication channel or offer protection against jamming. In civilian applications, this could allow reuse of the frequency band now used by television broadcasters, creating more bandwidth available for transmission.

Cristi, Fargues, and Hagstette have previously studied a similar problem in the context of a weak co-channel communication signal embedded within a strong terrestrial television broadcast signal [1]. They identified three possible schemes to separate the signals, namely blind source separation, using multiple antennas and Kalman filtering, and using adaptive noise cancellation. The first two were studied by Hagstette [2], [3] and Attique [4]. The adaptive noise cancellation approach is the focus of this study.

In these past studies, the television broadcast signal types considered followed the Advanced Television Systems Committee (ATSC) standard, used in North America, and the Digital Video Broadcasting–Terrestrial (DVB–T) standard, used in Europe, Africa, India, and others. Recently, Lai developed a Simulink model to generate signals following the Digital Terrestrial Multimedia Broadcasting (DTMB) standard used in People’s Republic of China [5]. Being a more recent standard, DTMB uses more advanced error correction and is more robust to Doppler shift distortion than previously adopted standards [6], [7]. In this study, the signals considered are a four–quadrature amplitude modulation (QAM) communication signal and a DTMB television broadcast signal. We assume the communication signal and DTMB signal transmitters are not co-located. The DTMB signal transmission channel has multiple paths, while the communication signal transmission channel has a single path and AWGN.

We implement a Simulink model of the proposed approach and present the schematic of the overall setup in Figure 1. The details of the preprocessor and adaptive noise canceler are shown in Figures 2 and 3. The DTMB television broadcast signal has well-known characteristics, good error correction and strong power. Known standard characteristics are taken advantage of to extract the weak communication signal using an adaptive noise cancellation scenario. The proposed signal extraction process has two phases. First, a preprocessor reconstructs the DTMB signal and minimizes the contribution of the DTMB signal in the received combined noisy signal. Second, an adaptive noise canceler is designed to recover the communication signal using the reconstructed DTMB signal as a reference.

Results show that the adaptive noise canceler requires a very accurate channel estimation process to recover the weak communication signal. Results also show that symbol error ratio (SER) levels below 10^{-4} may be obtained with up to 20% error in estimated transmission channel coefficients values when an exact length of the transmission channel is selected.

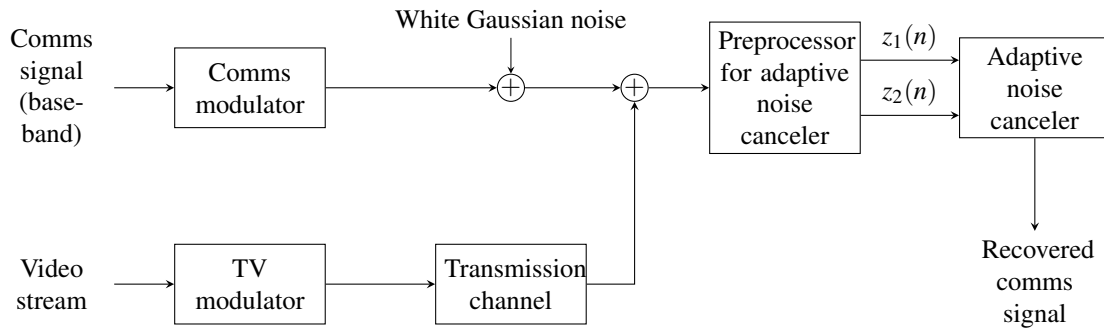


Figure 1. Schematic of overall setup.

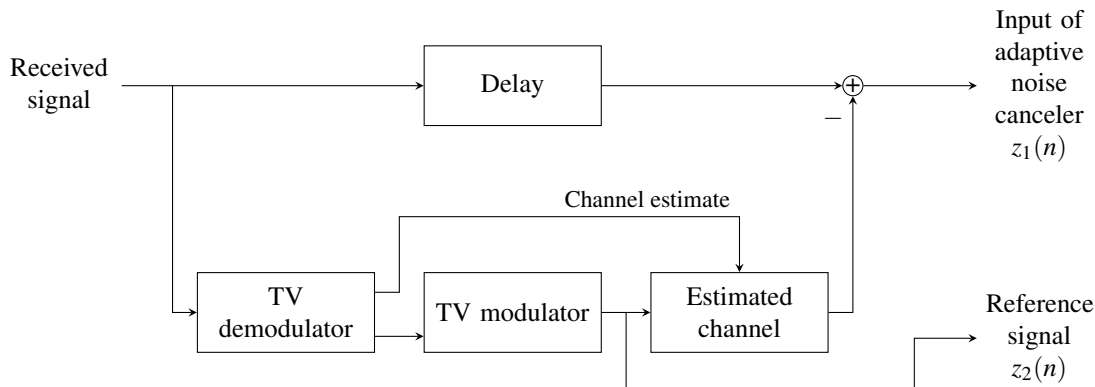


Figure 2. Preprocessor for adaptive noise cancellation, after [1].

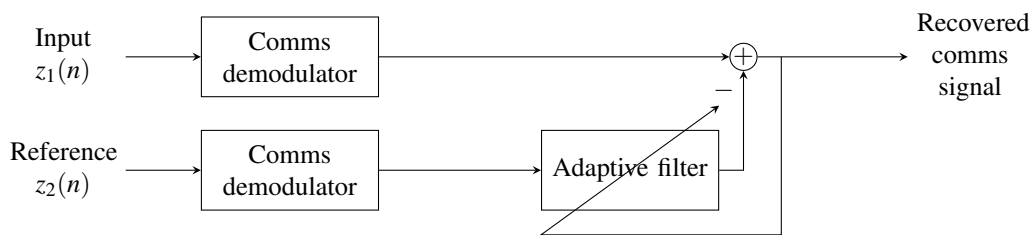


Figure 3. Adaptive noise canceler block, after [1].

List of References

- [1] R. Cristi, M. P. Fargues, and M. E. Hagstette, "Detection of a weak communication signal in the presence of a strong co-channel TV broadcast interferer," Oct. 2013, unpublished.
- [2] M. E. Hagstette, "Extraction of a weak co-channel interfering communication signal using complex independent component analysis," M.S. thesis, Dept. Elect. and Comput. Eng., Naval Postgraduate School, Monterey, CA, June 2013.
- [3] M. E. Hagstette, M. P. Fargues, and R. Cristi, "Extraction of a weak co-channel interfering communication signal using complex independent component analysis," in *Conf. Rec. 47th Asilomar Conf. Signals, Syst. and Comput.*, Pacific Grove, CA, Nov. 2013, pp. 1171–1175.
- [4] A. Sajid, "Detection of a low power communication signal in the presence of a strong co-channel TV broadcast interference using Kalman filter," M.S. thesis, Dept. Elect. and Comput. Eng., Naval Postgraduate School, Monterey, CA, Dec. 2014.
- [5] H.-C. Lai, "Simulink-based implementation and performance analysis of TDS-OFDM in time-varying environments," M.S. thesis, Dept. Elect. and Comput. Eng., Naval Postgraduate School, Monterey, CA, Sep. 2014.

- [6] J. Song, Z. Yang, L. Yang, K. Gong, C. Pan, J. Wang, and Y. Wu, "Technical review on Chinese digital terrestrial television broadcasting standard and measurements on some working modes," *IEEE Trans. Broadcast.*, vol. 53, no. 1, pp. 1–7, Mar. 2007.
- [7] R. Karamchedu. (2009, May 4). Does China have the best digital television standard on the planet? [Online]. Available: <http://spectrum.ieee.org/consumer-electronics/standards/does-china-have-the-best-digital-television-standard-on-the-planet/0>

Acknowledgments

I wish to take this opportunity to thank my wife, Doreen, for taking care of the household so that I may concentrate on my studies. I would not be able to do this without you.

To our daughter, Megan, thank you for coming into our life. Your smiles and laughter make all the trouble worthwhile and we hope you can continue to smile and laugh as you grow up.

To my thesis advisors, Professor Fargues and Professor Cristi, thank you for your help in doing up this thesis. You gave me many hours of your time to go through the work, cleared up many doubts along the way and encouraged me when I tripped over obstacles. I am certainly glad to have you as my advisors.

THIS PAGE INTENTIONALLY LEFT BLANK

CHAPTER 1:

Introduction

The motivation for the thesis, past work, approach followed, and thesis organization are discussed in this chapter.

1.1 Motivation

In this thesis, we consider a scenario where a weak signal such as a communication signal is embedded within a much stronger signal such as a television broadcast signal in the same frequency band, as shown in Figure 1.1. Since both signals overlap the same frequency band, they cannot be separated by filtering in the frequency domain. An adaptive filter approach to recover a weak narrowband communication signal embedded in a strong wideband television broadcast signal and additive noise is investigated by taking advantage of the known characteristics of the television broadcast signal standard. This could have both military and civilian applications if successful. For instance, in the military, this could be used to create a covert communication channel or offer protection against jamming. In civilian applications, this could allow for reuse of the same frequency band and more bandwidth available for transmission.

1.2 Past Work

Radio frequency is a limited resource. To maximize the use of this limited resource, one of the techniques used by communication systems is frequency reuse. Often, frequency reuse results in co-channel interference, limiting performance [1]. There has been much research conducted to resolve co-channel interference in areas such as cellular communications and satellite communications [2]–[6].

Cristi, Fargues, and Hagstette have previously studied a similar problem in the context of a weak co-channel communication signal embedded within a strong terrestrial television broadcast signal [7]. They identified three possible schemes to separate the signals, namely blind source separation, using multiple antennas and Kalman filtering, and using adaptive noise cancellation. The first two were studied by Hagstette [8], [9] and Attique [10]. The

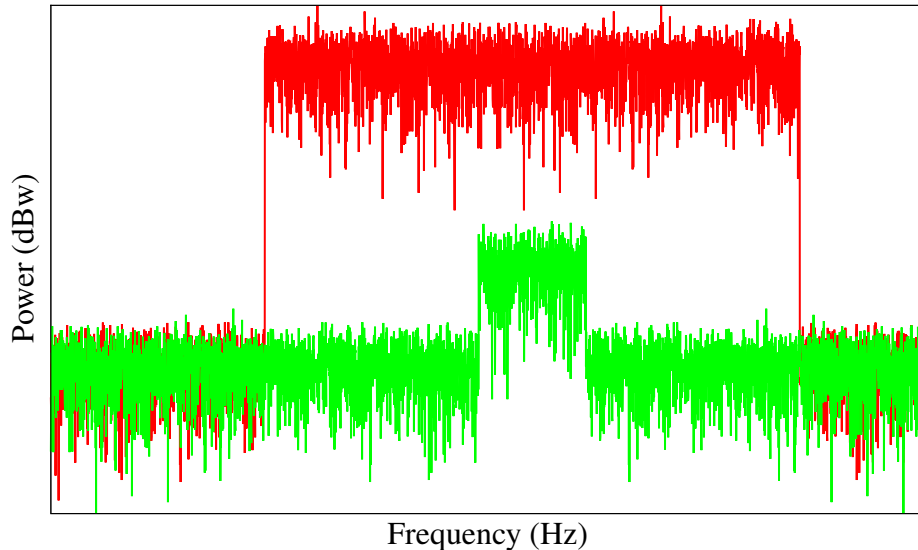


Figure 1.1. Plot showing a weak co-channel communication signal (green) embedded within a strong television broadcast signal (red).

third approach of using adaptive noise cancellation is the focus of this study.

In these previous studies, the television broadcast signal types considered followed the Advanced Television Systems Committee (ATSC) standard, used in North America, and the Digital Video Broadcasting–Terrestrial (DVB–T) standard, used in Europe, Africa, India, and others, as seen in Figure 1.2. These television standards were developed in the 1990s. Recently, Lai developed a Simulink model to generate signals following the Digital Terrestrial Multimedia Broadcasting (DTMB) standard used in China [11]. The DTMB standard was adopted as a national standard of People’s Republic of China in 2007 [12]. Being a more recent standard, DTMB uses more advanced error correction and has a better performance with respect to Doppler shift than previously adopted standards [13], [14]. These advantages allow for easier signal reconstruction during demodulation and also make the adaptive noise cancellation step easier to implement.

1.3 Approach

In this study, we consider a four–quadrature amplitude modulation (QAM) signal to represent the weak communication signal and a DTMB signal to represent the strong signal. A 4–QAM signal was selected to represent a typical digital communication signal. As men-

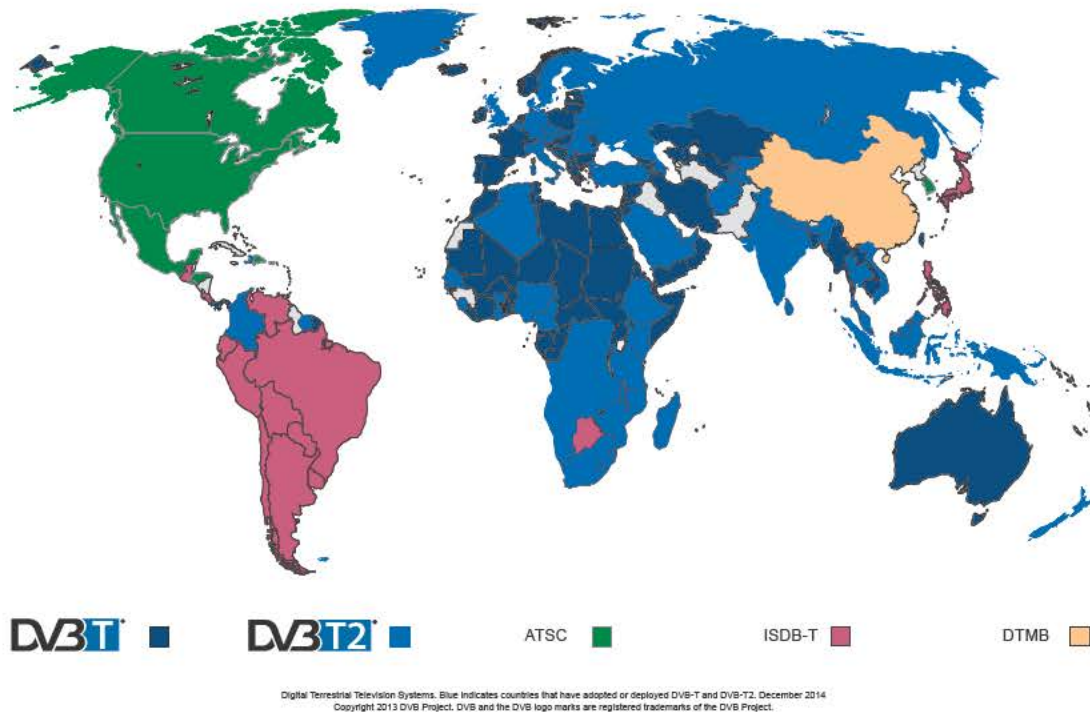


Figure 1.2. Areas of the world where ATSC, DVB–T and DTMB are used, from [15].

tioned earlier, the DTMB signal is chosen because its model is readily available from past work, and the standard is known to have better performance than older standards [14]. We test the setup with a simulation model in Simulink.

1.4 Thesis Organization

In Chapter 2, we provide the theoretical background needed to understand the method used in this thesis. In Chapter 3, we illustrate the method and its implementation in Simulink. In Chapter 4, we present the results obtained. In Chapter 5, we provide conclusions and recommendations for future work. In Appendixes A and B, we show the MATLAB code and the Simulink models used in the simulation. In Appendix C, we present additional plots to supplement the information provided in Chapter 4.

THIS PAGE INTENTIONALLY LEFT BLANK

CHAPTER 2: Theoretical Background

In this chapter, we first present a brief introduction to adaptive noise cancellation. Next, we discuss the structure of a DTMB signal and channel estimation for a DTMB signal.

2.1 Adaptive Noise Cancellation

Adaptive noise cancellation has been used to remove unwanted interference from signals in numerous applications. Some of the earlier applications are used in the removal of unwanted interference in electrocardiograms, canceling noise in speech signals, or removing antenna sidelobe interference. The unwanted interference could be the 60 Hz from the power line in a patient's electrocardiogram, the mother's own electrocardiogram in a fetus's electrocardiogram, engine noise in a pilot's speech, or an unwanted signal coming from the sidelobes in an antenna [16], [17].

A typical structure of a basic adaptive noise canceler is shown in Figure 2.1. The sensor input has the signal $s(n)$ and an uncorrelated noise $v_1(n)$ corrupting the signal. We desire to remove the noise $v_1(n)$ from the signal. A second sensor provides a reference for the noise $v_2(n)$, which is correlated with the noise $v_1(n)$. The aim of the filter is to take advantage of the correlation between $v_1(n)$ and $v_2(n)$ to produce an output $y(n)$ such that $y(n) = v_1(n)$. After subtraction, the error signal $e(n)$ will be the signal $s(n)$ [16].

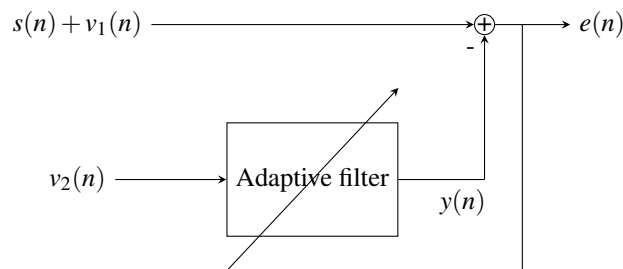


Figure 2.1. Typical structure of a basic adaptive noise canceler, after [18].

2.2 Structure of DTMB Signal

A DTMB signal is transmitted in frames and is based on orthogonal frequency-division multiplexing (OFDM). The most fundamental frame is the signal frame. As shown in Figure 2.2, the signal frame is made up of a frame header and a frame body with a baseband symbol rate of 7.56 mega symbols per second. The frame body has exactly 3780 symbols. The frame header, however, could have a length of 420, 595, or 945 symbols, depending on applications. In general, longer frame headers have a lower throughput but higher resilience to adverse conditions. In Figure 2.3, we can see the structure for the frame header of different lengths. Frame headers with a length of 420 and 945 symbols have a pre-amble, a pseudo-noise sequence, and a post-amble. Frame headers with a length of 595 symbols have only pseudo-noise sequence and no pre- and post-ambles. In particular, note that the pseudo-noise sequences can be used as pilot symbols to perform channel equalization as they are known at the receiver side [13], [19].

2.3 Channel Estimation for DTMB Signal

In this section, we focus on one aspect of DTMB modulation and demodulation—channel estimation. Transmission channel characteristics have a direct impact on signals propagating through them. We can model the channel impact as a linear filter with impulse response $h(n)$. The impulse response $h(n)$ is known as the channel impulse response (CIR). We want to undo the impact of the channel on the signal at the receiver so that we can correctly interpret the signal. The removal of the transmission channel distortion on the signal is known as channel equalization. Typically, the first step to channel equalization is to estimate the CIR, that is, channel estimation.

A DTMB signal is transmitted in frames, as mentioned in Section 2.2. There are pseudo-noise sequences within the frame header that are known to the receiver. The receiver can use these predetermined symbols as pilot symbols to perform channel estimation [20], [21].



Figure 2.2. Structure of a DTMB signal frame, from [13].

Pre-amble (82)	Pseudo-noise sequence (255)	Post-amble (83)
----------------	-----------------------------	-----------------

(a) Frame header of length 420 symbols.

Pseudo-noise sequence (595)

(b) Frame header of length 595 symbols.

Pre-amble (217)	Pseudo-noise sequence (511)	Post-amble (217)
-----------------	-----------------------------	------------------

(c) Frame header of length 945 symbols.

Figure 2.3. Frame headers of various length. The number in parenthesis denotes the number of symbols, after [13], [19].

The estimated channel frequency response $\hat{H}(f)$ can be calculated by

$$\hat{H}(f) = \frac{Y_{pilot}(f)}{X_{pilot}(f)} \quad (2.1)$$

where $X_{pilot}(f)$ is the transmitted pilot sequence in the frequency domain and $Y_{pilot}(f)$ is the received pilot sequence in the frequency domain.

The estimated CIR $\hat{h}(n)$ can then be found from

$$\hat{h}(n) = \text{IFFT} [\hat{H}(f)] \quad (2.2)$$

where $\text{IFFT}[\cdot]$ denotes the inverse fast Fourier transform (FFT) operation.

The calculation of $\hat{H}(f)$ using (2.1), however, runs a risk of division by zero, particularly when the quantity $X_{pilot}(f)$ is small.

To improve the numerical stability, we note that

$$\begin{aligned} \frac{1}{X_{pilot}(f)} &= \frac{1}{X_{pilot}(f)} \frac{X_{pilot}^*(f)}{X_{pilot}^*(f)} \\ &= \frac{X_{pilot}^*(f)}{|X_{pilot}(f)|^2} \\ &\approx \frac{X_{pilot}^*(f)}{|X_{pilot}(f)|^2 + \epsilon} \end{aligned} \quad (2.3)$$

where $X_{pilot}^*(f)$ is the complex conjugate of $X_{pilot}(f)$ and ε is a small number.

The small number ε added to the denominator of (2.3) is designed to improve the numerical stability of the division.

Substituting (2.3) into (2.1), we get

$$\hat{H}(f) = \frac{Y_{pilot}(f)X_{pilot}^*(f)}{|X_{pilot}(f)|^2 + \varepsilon}. \quad (2.4)$$

By using (2.4) to calculate $\hat{H}(f)$, we get improved numerical stability in the estimation of the transmission channel frequency response, especially when the quantity $X_{pilot}(f)$ is very small. This in turn ensures the estimated CIR is numerically better approximated.

CHAPTER 3:

Methodology

The adaptive noise cancellation process implemented to extract the communication signal embedded in the television broadcast signal is discussed in this chapter. The methodology was developed by Cristi and used in this thesis with permission [7].

3.1 Schematic of Overall Implementation

In Figure 3.1, we show a schematic of the overall setup. On the left, we generate a 4-QAM communication signal and a DTMB television broadcast signal. The communication channel has additive white Gaussian noise (AWGN) and the television broadcast signal passes through a transmission channel. The received signal undergoes preprocessing, as discussed in Section 3.2, followed by adaptive noise cancellation, as discussed in Section 3.3. We then recover the communication signal and compare against the transmitted version to compute the symbol error ratio (SER).

3.2 Preprocessing for Adaptive Noise Cancellation

In Section 2.1, we noted that, for the basic adaptive noise cancellation, we need the signal that has been corrupted with noise $s(n) + v_1(n)$ and a reference noise $v_2(n)$. In our context, the television broadcast signal is considered as the noise, and the communication signal is the signal-of-interest. In our application, we only have the combined signal where the communication signal is embedded within the television signal. We now discuss the process to

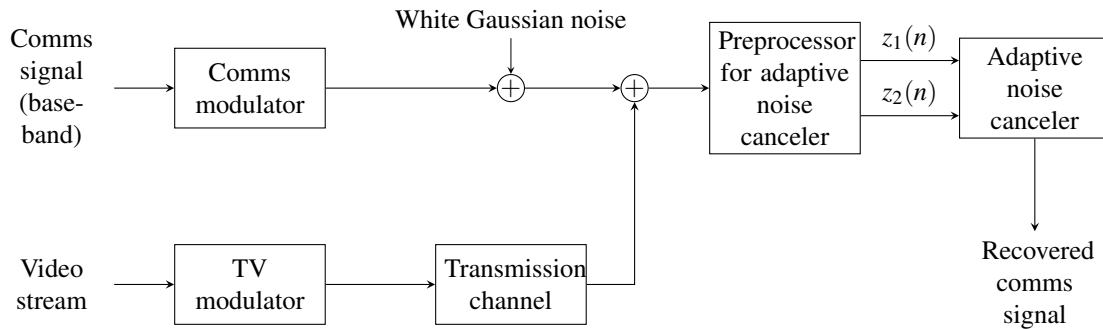


Figure 3.1. Schematic of overall setup.

obtain a reference noise signal from the combined signal.

In Figure 3.2, we show the preprocessor for adaptive noise cancellation. The received signal contains the communication signal embedded in the television broadcast signal. In the upper path, we perform a first cancellation through the upper path using the estimated channel. The delay in the upper path is added to synchronize the signal due to computational delays in the lower path. In the lower path, the received signal passes through the TV demodulator to obtain the baseband TV signal and the estimated CIR. The baseband TV signal is then re-modulated into the television broadcast signal. The reconstructed television broadcast signal is filtered through the estimated channel and is subtracted from the received signal (first cancellation) to compute the signal $z_1(n)$. The adaptive noise cancellation process, therefore, only needs to cancel the remaining noise due to the channel estimation error. The reconstructed television broadcast signal is also passed to the adaptive noise canceler as the reference signal $z_2(n)$.

3.3 Adaptive Noise Cancellation

In Figure 3.3, we show the details of the adaptive noise canceler. Since the final goal is to reconstruct the communication signal in baseband, the two signals $z_1(n)$ and $z_2(n)$ passed from the preprocessor are first demodulated to baseband. Then they are used as the input and reference to the adaptive noise canceler. At the output, we recover the baseband communication signal.

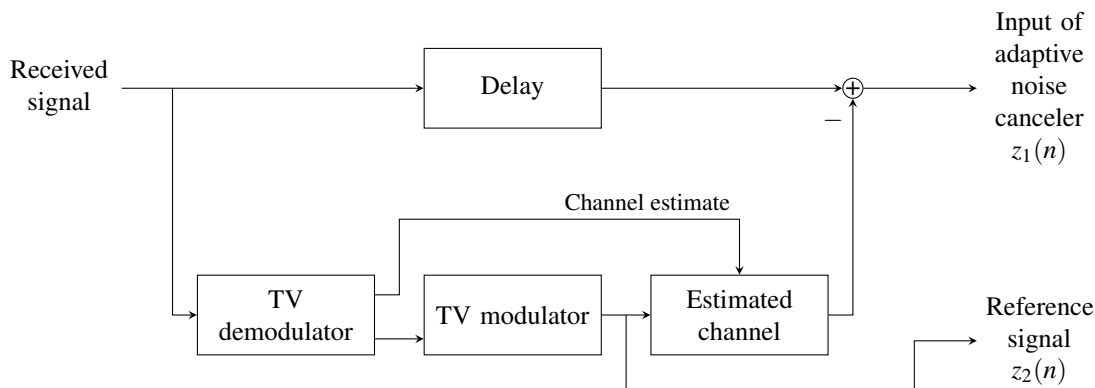


Figure 3.2. Preprocessor for adaptive noise cancellation, after [7].

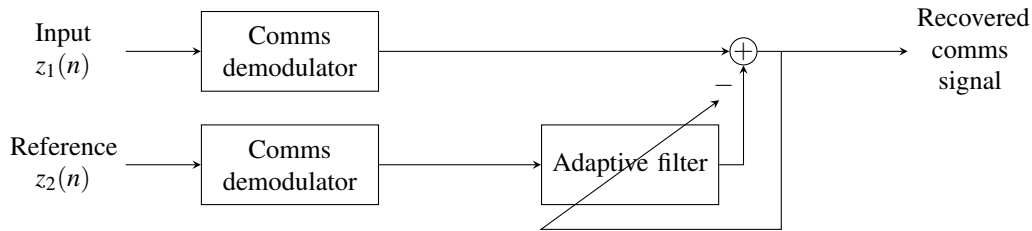


Figure 3.3. Adaptive noise canceler block, after [7].

3.4 Simulink Implementation

We implement the discussed model in Simulink with the differences described in the following sections. The detailed Simulink model and MATLAB code are shown in appendixes A and B.

3.4.1 Replacement of Modulator and Demodulator

The reference signal $z_2(n)$ is generated by demodulating the received television broadcast signal and remodulating it in the preprocessor for the adaptive noise cancellation, as shown in Figure 3.2. We can still recover the television broadcast signal despite the interference caused by the communication signal by taking advantage of the error correction in the television broadcast signal. In the Simulink implementation, we do not have the television broadcast signal demodulator and modulator blocks because they add an additional level of complexity to the model. By not implementing the demodulator and modulator, we eliminate potential sources of error coming from the demodulator and modulator. In this work, we assume the television broadcast signal can be recovered with 100% accuracy due to the superior error correction coding in DTMB [14].

In place of the television demodulator and modulator, we implement only the channel estimator of the demodulator. The actual television broadcast signal from the transmitter is routed into the preprocessor to replace the output from the modulator. See Figure 3.4 for the Simulink implementation of the preprocessor.

3.4.2 Inclusion of Blocks to Calculate Error Rate

For the purpose of quantifying the performance of the scheme, we examine the SER for a given signal-to-noise ratio (SNR). We include in the Simulink implementation the means to calculate the SER for the simulation runs.

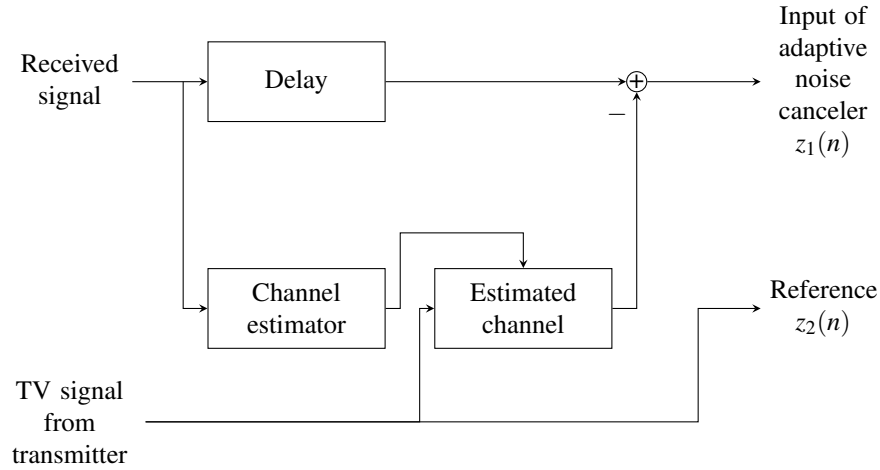


Figure 3.4. Simulink implementation of the preprocessor.

3.5 Simulations

In this study, we investigate the ability to recover the low-power communication signal using adaptive noise cancellation under the following conditions.

1. The television broadcast signal is assumed to be a DTMB signal. The weak communication signal is a 4-QAM signal.
2. The television broadcast signal and communication signal are random binary bit-streams.
3. The television broadcast transmitter and the communication transmitter are not co-located. The television broadcast signal and the communication signal pass through different transmission channels to arrive at the receiver. The transmission channel of the television broadcast signal has multipaths, while the communication signal goes through a single path with AWGN.
4. We investigate the capabilities of the proposed approach to recover the weak communication signal as the AWGN power varies. We define two power ratio quantities—interference-to-noise ratio (INR) and signal-to-interference ratio (SIR)—given by

$$\text{INR} = \frac{\text{Weak communication signal power}}{\text{AWGN power}} \quad (3.1)$$

and

$$\text{SIR} = \frac{\text{Television broadcast signal power}}{\text{Weak communication signal power}}. \quad (3.2)$$

Throughout the study, we maintain a fixed SIR level equal to 30 dB. This specific level is selected to be consistent with past studies [8].

3.5.1 Simulation Parameters for Television Broadcast Signal

The television broadcast signal is based on the DTMB standards and is generated using the model developed by Lai [11]. The simulation parameters selected for the DTMB signal are shown in Table 3.1. The DTMB signal has a frame header of 420 symbols. Within the frame header, the pseudo-noise sequence has a length of 255 symbols which are used for channel estimation in this study. The total frame length is equal to 4200 symbols. The sampling rate F_s is equal to 7.56 MHz to be in line with standard broadcasting applications [11].

Table 3.1. Simulation parameters for television broadcast signal, after [11].

Description	Value
Sampling rate F_s	7.56 MHz
Length of frame	4200 symbols
Length of frame header	420 symbols
Length of pilot symbols	255 symbols

3.5.2 Simulation Parameters for Communication Signal

The communication signal is a 4-QAM communication signal. In Table 3.2, we list the simulation parameters. The carrier frequency and data rate of the signal are chosen such that they are an integer division of the sampling rate F_s . This selection was made so that the sampling period can become the step size used in the simulation. Note that the fundamental sample time would be reduced, slowing down the simulation, if the carrier frequency and data rate are not integer divisions of the sampling rate F_s [22].

Table 3.2. Simulation parameters for the communication signal.

Description	Value
Carrier frequency	$\frac{F_s}{10}$
Data rate	$\frac{F_s}{100}$

3.5.3 Simulation Parameters for Multipath Channel

The television broadcast signal passes through a multipath channel to get to the receiver. To be consistent with past studies [7], the multipath channel has three paths with characteristics shown in Table 3.3. As a result of the sampling rate F_s and the length of the longest path, we need a filter length of 17 to model the multipath transmission channel.

Table 3.3. Characteristics for the multipath channel.

	Delay (samples / μ s)	Power (dB)
Path 1	0 / 0	0
Path 2	10 / 1.32	-10
Path 3	15 / 1.98	-15

3.5.4 Simulation Parameters for Adaptive Filter

In Table 3.4, we show the characteristics of the adaptive filter used in the adaptive noise cancellation. We choose a normalized-least-mean-square (NLMS) adaptive filter for its simplicity, robustness, and ability to track changes in the signal due to possible changes in the transmission channel [23]. The length of the filter is selected to be large enough to model the characteristics of the multipath channel. The step size is selected through trial and error to get reasonable performance from the adaptive noise canceler. The filter weights are arbitrarily initialized to zero at the beginning of the simulation.

Table 3.4. Characteristics for the NLMS adaptive filter.

Description	Value
Filter length	50
Step size	0.0001
Initial filter weight	0

CHAPTER 4:

Results and Discussions

In this chapter, we present the simulation results obtained. The ability of the entire scheme to recover the weak communication signal is evaluated by examining the SERs across different INRs.

4.1 Need for Multiple Trials

Typically, the SER is expected to decrease monotonically as the signal-to-noise ratio increases [24]. In Figure 4.1, we show the results from a single simulation run obtained for a transmission length of 42000 symbols for each INR. The SER does not decrease monotonically with increasing INR as expected. Hence, multiple runs are needed to provide statistically meaningful results. In Figure 4.2, we present the results obtained by averaging over 100 trials. In Figure 4.2a, the lower and upper ends of the error bars represent the 5th and 95th percentile levels, respectively. We note that, other than the case where the INR is equal to 5 dB, there are more than 50% of the SER values that are equal to zero for each INR, as seen in Figure 4.2b. To allow us to plot such values onto the logarithmic axis, they are represented as 10^{-7} in the plot. The non-zero SER values, therefore, skew the mean SER upwards, since more than 50% of the SER values are equal to zero. We note that, since more than 50% of the SER values are equal to zero, the median SER is zero.

Increasing the number of trials helped to produce more statistically meaningful results. It also, however, lengthened the time required to produce results significantly. For instance, on an Intel Xeon computer available in our laboratory, a single run where 42000 symbols were transmitted took about 0.25 h. Generating the complete SER curve over a range of INRs between -5 dB and 50 dB at 5 dB interval took about 3 h.

To reduce the computational impact, we used the Parallel Computing Toolbox in MATLAB to enable parallel processing within a Intel Xeon 6-core computer. This allowed us to obtain a six-fold reduction in processing time. For example, the time required for the complete SER curve over the same range of INRs was reduced from 3 h to 0.5 h. The time reduction allowed us to perform multiple trials within a more realistic length of time. For

instance, 100 trials could be completed in 50 h with parallel computing instead of 300 h without parallel computing. Despite the six-fold decrease in processing time achieved with parallel computing, the long processing time, nevertheless, imposed a practical limit on the simulations.

For the rest of this chapter, the average SERs shown are calculated over 100 trials. The error bars, if shown, show the range covered from the 5th percentile to 95th percentile SER values.

4.2 Effect of Number of Coefficients in Channel Estimate

The channel estimator in the preprocessor provides the estimated CIR $\hat{h}(n)$ through an inverse-FFT operation. The number of coefficients in $\hat{h}(n)$ is determined by the size of the FFT. In most practical implementations, not all the coefficients are significant. The non-significant coefficients contribute to noise [25]. In Lai's implementation of the channel estimator, the number of significant coefficient was assumed to be at most 165, and the remaining coefficients were regarded as noise [11]. Since the channel estimator is derived from her work, the channel estimator in this study works in a similar fashion.

We first investigate the effect of the number of coefficients in the CIR has on the resulting SER. The true transmission channel has 17 coefficients. To remove the effect of the transmission channel completely, the channel estimator must have at least the same number of coefficients as the transmission channel, that is, 17 coefficients.

We keep the first k coefficients that come out of the channel estimator and truncate the rest. Since the channel estimator produces at most 165 coefficients, k is selected such that $0 \leq k \leq 165$. In Figure 4.3, we show the SER as a function of the INR for different values of k . When $k = 17$, the channel estimator has exactly the same number of coefficients as the actual transmission channel. We denote this scenario as 1x. When $k = 85$, the channel estimator has five times more coefficients than the actual transmission channel. We denote this scenario as 5x. Similarly, the scenario whereby $k = 165$ is denoted as 9x, rounded to one significant figure. Results show that the SER degrades when the length of the estimated CIR $\hat{h}(n)$ is higher than that of the true transmission channel. In Figure 4.4, we plot the mean SERs with their error bars for each value of k . The variation in the data tends to

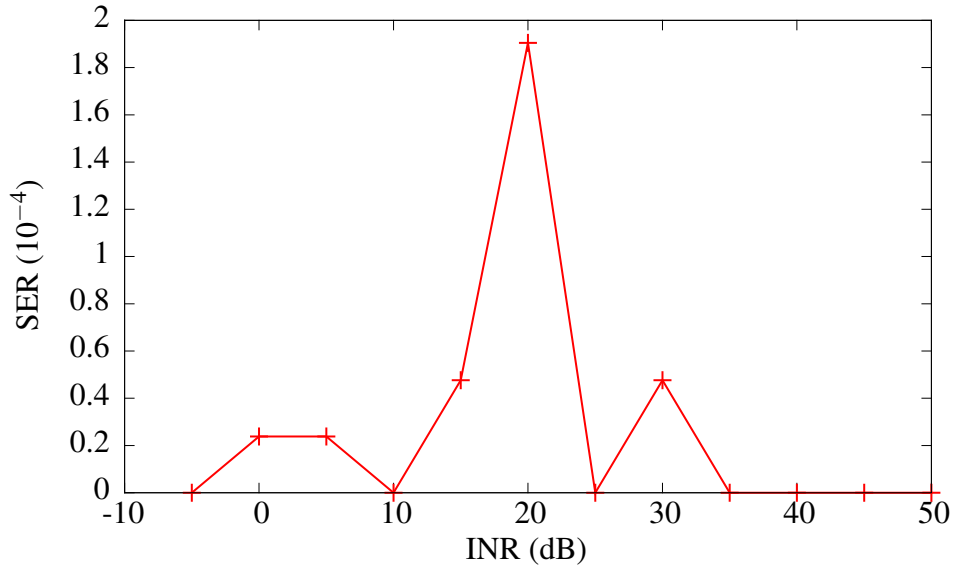


Figure 4.1. Plot of SER against INR with 42 000 symbols transmitted per INR.

increase for higher values of k .

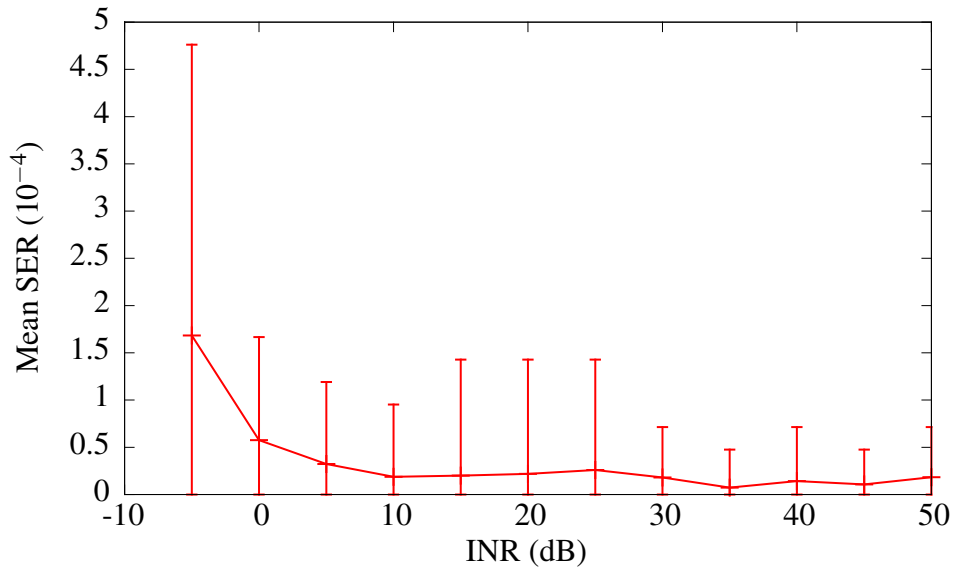
This behavior is likely due to the limitation in the estimation process for the CIR. A typical estimated CIR made by the channel estimator is shown in Figure 4.5. There are only a small number of significant coefficients. The non-significant coefficients are non-zero due to the limitation in the estimation process. Note that, when too many coefficients are used, the noise in these non-zero coefficients are accumulated and results in significant errors in the estimated television signal. As a result, the adaptive noise canceler is not able to recover the communication signal. This result also shows that a good channel estimator is important in this scheme. The channel estimator must not only be able to accurately estimate the coefficients itself but also must be able to remove the non-significant coefficients due to the estimation process [25].

4.3 Effect of Error in Channel Coefficients

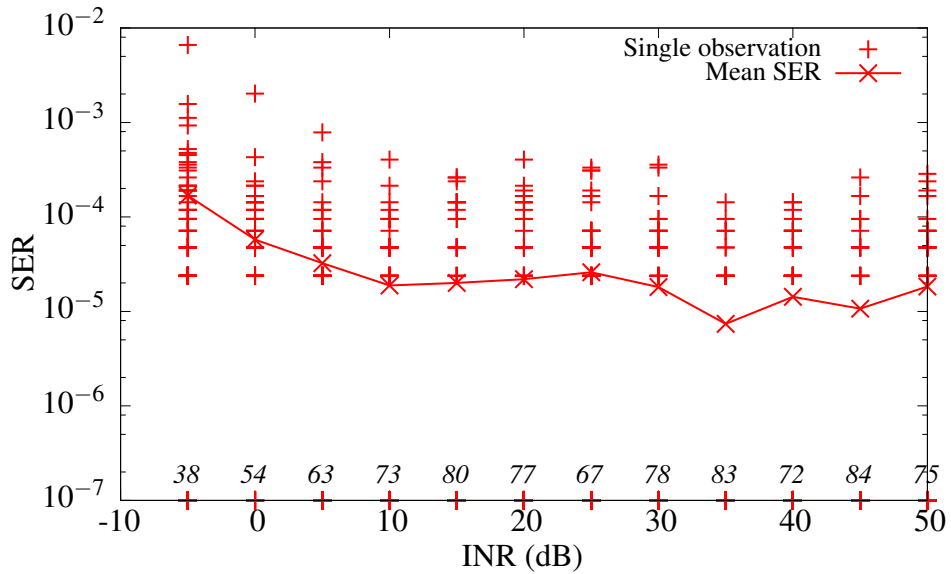
In this section, we first assume there is no error in the length of the estimated CIR $\hat{h}(n)$. The only source of error in $\hat{h}(n)$ is due to errors in the coefficient values. We run the simulation for 5%, 10%, and 20% errors in the estimated channel coefficients and observe the corresponding SERs.

The plots of SER against different INRs are shown in Figure 4.6. The 5th and 95th percentiles are shown as error bars in Figure 4.7. In some instances, the SERs are equal to zero. To allow us to plot such values onto the logarithmic axis, they are represented as 10^{-7} in the plot. In general, the SER increases as the percentage of error in the channel coefficients increases. There are occasions where the SER appears to increase when INR increases, such as from 20 dB to 25 dB in Figure 4.7b and 4.7c, respectively. This is attributed to the large outliers in the associated SER. In particular, note that for 5% and 10% error at greater than 10 dB, there appears to be no error bar. Note that, in these cases, fewer than 5% of the SERs values are nonzero. That is, at least 95% of the SERs are equal to zero. The outliers beyond the 95th percentile increased the mean SER. The median SERs for these cases are zero. The distribution of SER values for each INR illustrates this skewed behavior and is presented in Appendix C.

The SERs at the highest percentage error of 20%, however, remain below 10^{-4} for INRs greater than 0 dB. This shows that, with an appropriate channel estimation process, the approach can recover the weak communication signal with a good SER.



(a) Plot of mean SER against INR with 42 000 symbols transmitted per INR over 100 trials. The lower and upper ends of the error bars show the 5th and 95th percentiles, respectively.



(b) Plot of SER against INR with 42 000 symbols transmitted per INR over 100 trials. Each cross shows a single observation of the SER at a particular INR. SER values equal to zero are represented as 10^{-7} on the logarithmic axis. The numbers in italics just above the x -axis indicate the number of trials with SERs equal to zero at a given INR level.

Figure 4.2. Plot of SER against INR with 42 000 symbols transmitted per INR over 100 trials.

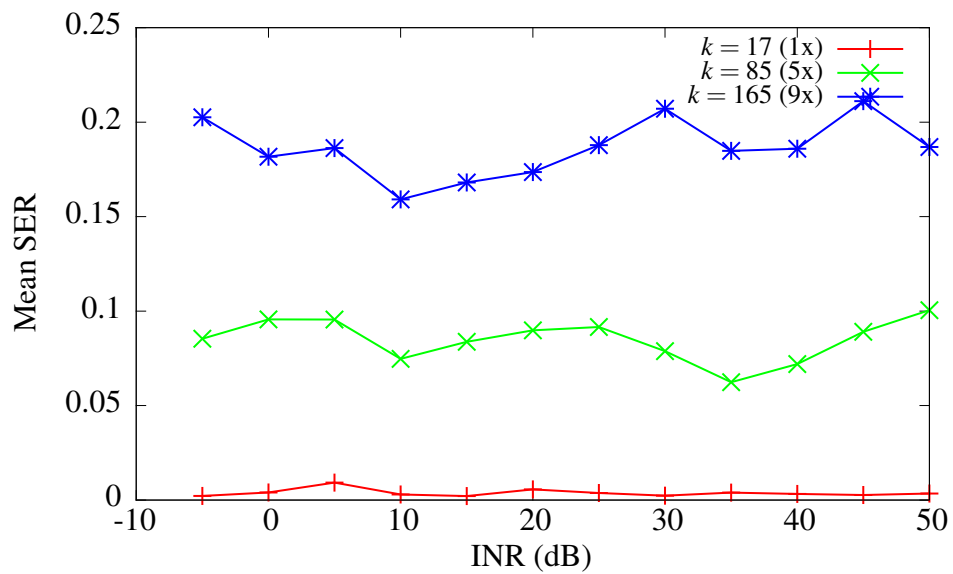


Figure 4.3. Plot of mean SER against INR with different number of coefficients k in the estimated CIR averaged over 100 trials. The number in parenthesis represents the increase in the number of coefficients used in the estimated CIR as compared to the true transmission channel.

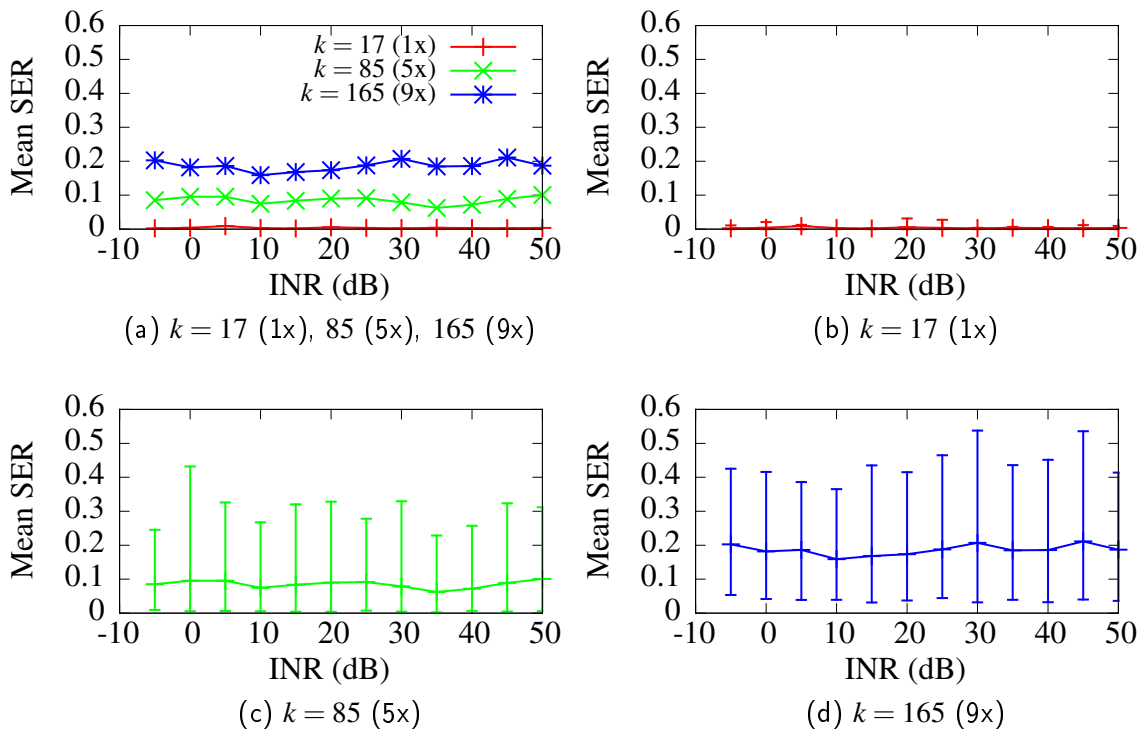


Figure 4.4. Plot of mean SER against INR for different number of coefficients k in the estimated CIR averaged over 100 trials with error bars. The error bars show the range covered from the 5th percentile to 95th percentiles. The y-axis range in all plots is kept constant for comparison. (a) Mean SER for $k = 17$ (1x), 85 (5x), and 165 (9x). (b)–(d) Mean SER and 90% confidence intervals for listed values of k .

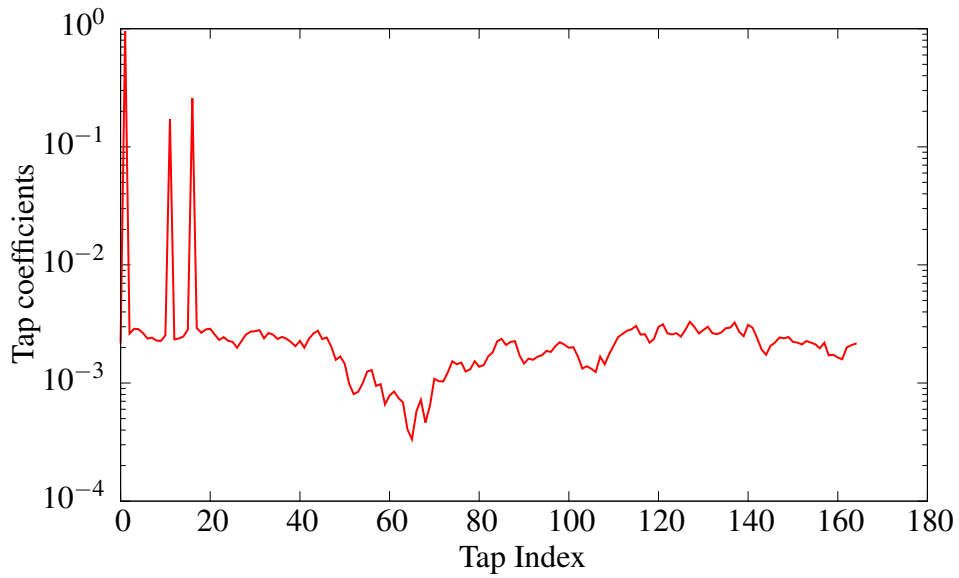


Figure 4.5. Typical plot of estimated CIR $\hat{h}(n)$.

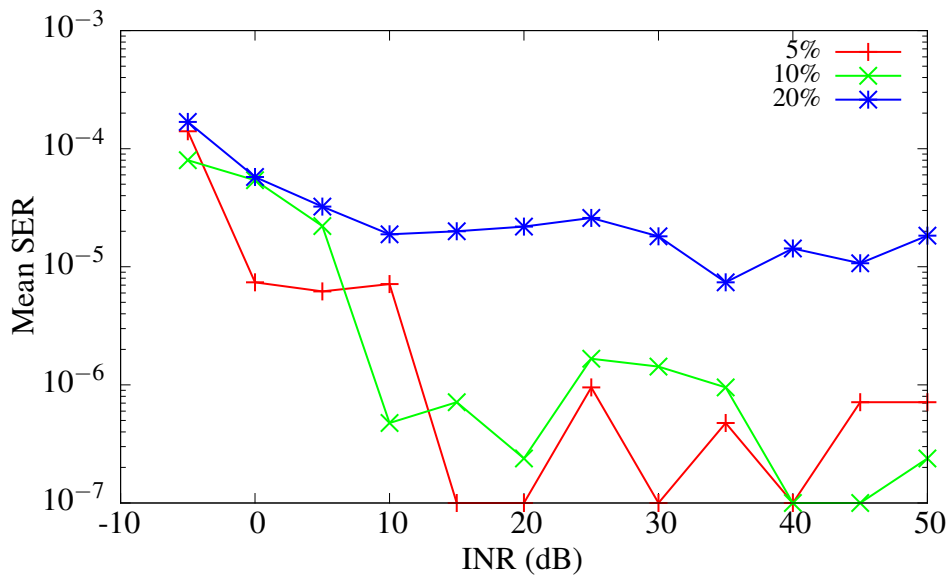


Figure 4.6. Plot of mean SER against INR for different errors in estimated channel coefficients averaged over 100 trials. SER values equal to zero are represented as 10^{-7} in the logarithmic axis.

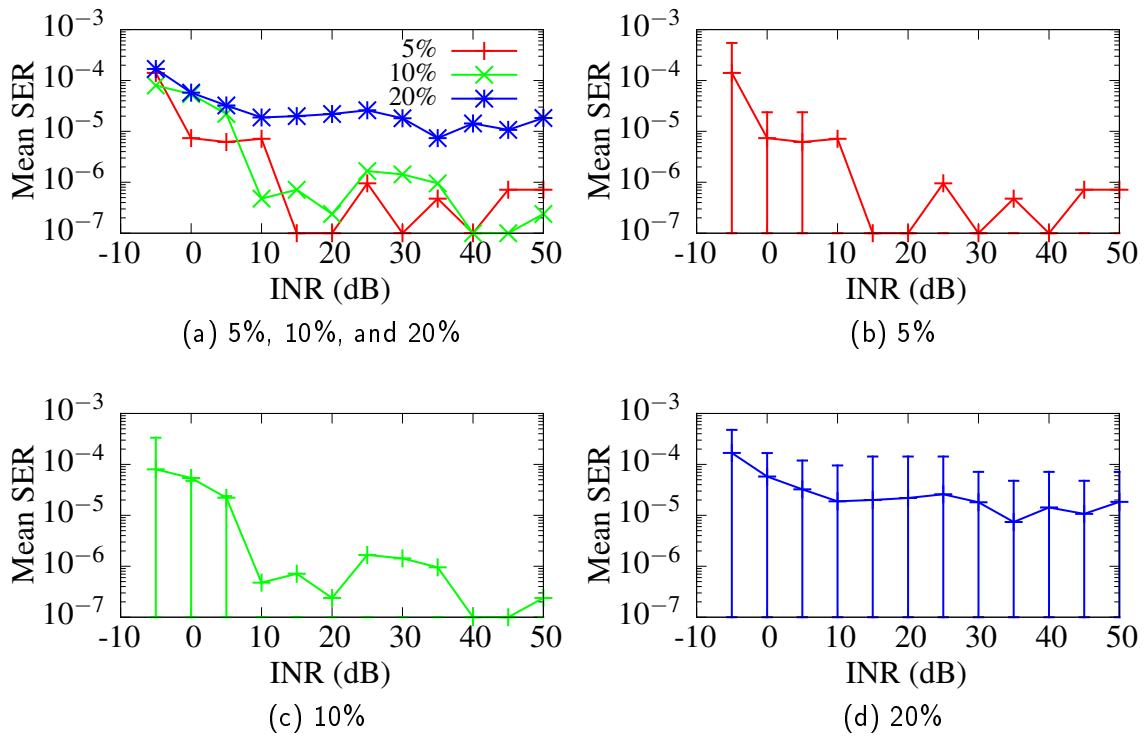


Figure 4.7. Plot of mean SER against INR for different errors in estimated channel coefficient values averaged over 100 trials with error bars. (a) Mean SER for 5%, 10%, and 20% errors in channel coefficients. (b)–(d) Mean SER and 90% confidence intervals for listed errors in channel coefficients.

THIS PAGE INTENTIONALLY LEFT BLANK

CHAPTER 5:

Conclusions

In this chapter, we give a summary of the results obtained and suggest recommendations for future work.

5.1 Summary

We implemented a Simulink model to examine the performance of an adaptive noise canceler to recover a weak 4-QAM communication embedded in a strong DTMB television broadcast signal. We successfully integrated the DTMB signal generator with the communication signal generator, transmission channel, the preprocessor and the adaptive noise canceler to form a working Simulink model. Noting the long processing time, we implemented parallel computing and achieved a six-fold reduction in the processing time. Using the resulting model, we tested the adaptive noise canceler under different scenarios. Results showed that the adaptive noise canceler required a very accurate channel estimation process to recover the weak communication signal. With the correct number of channel coefficients, the adaptive noise canceler could cope with at least up to 20% error in channel coefficients to produce SERs of the order of magnitude 10^{-4} .

5.2 Recommendations for Future Work

The following recommendation for future work is derived from some questions arising from this study.

- This study considered the ability of the adaptive noise canceler to recover a 4-QAM communication signal embedded in a strong DTMB television broadcast signal. Possible future work could study the performance of the adaptive noise canceler with other television broadcast signals e.g., ATSC or DVB-T.
- The channel estimator used in this study is only one of the possible channel estimator approaches available for DTMB. For example, Zhang proposed an iterative channel estimator scheme [21]. A possible future work could investigate whether the adaptive noise canceler would work with other types of channel estimator.

- The long processing time noted in the study was partially mitigated using parallel computing across multiple cores within a single machine. Future work could attempt to further reduce the processing time by distributing the computational workload across a computing cluster instead of a single machine or to implement the model in a compiled language such as C.

APPENDIX A: Simulink Models

In this appendix, we show the detailed Simulink models used in this study.

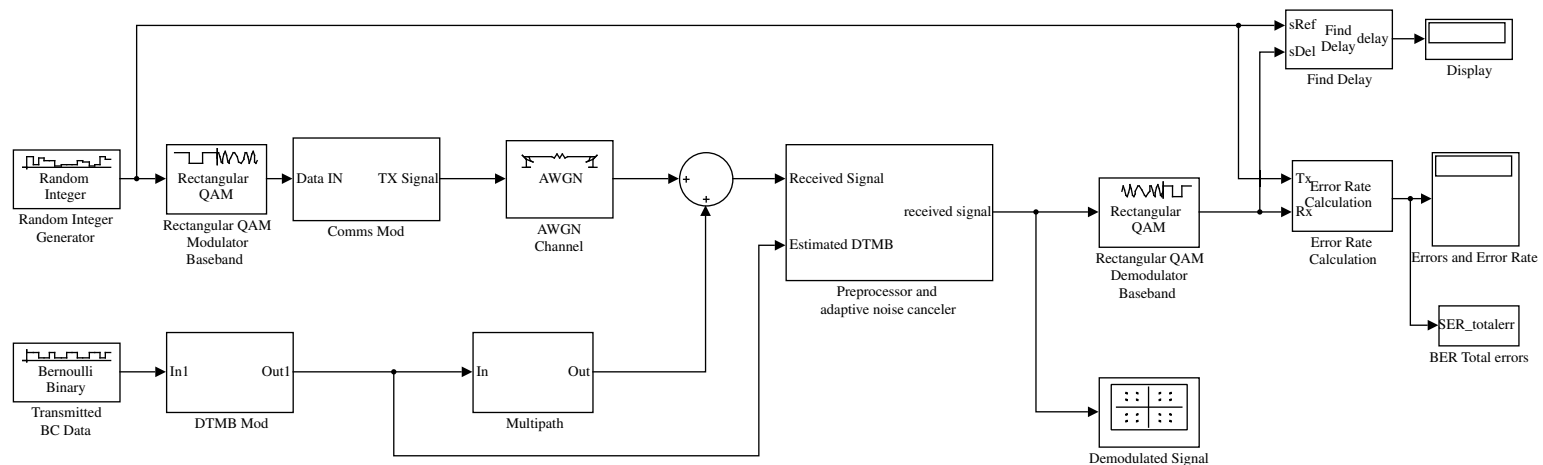


Figure A.1. Overall Simulink model. The detailed models for the communication signal modulator, DTMB modulator, multipath channel, preprocessor and adaptive noise canceler are shown in Figures A.2 to A.5.

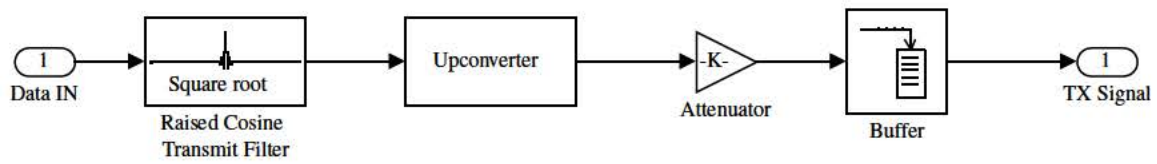


Figure A.2. Simulink model for communication signal modulator.

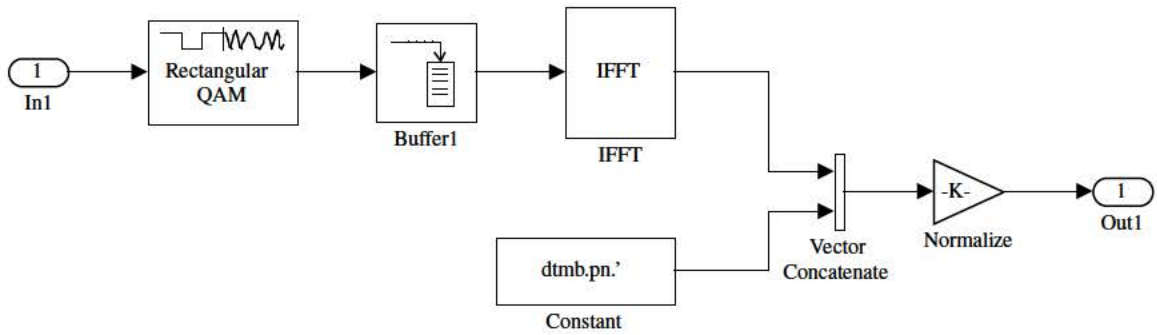


Figure A.3. Simulink model for DTMB modulator.

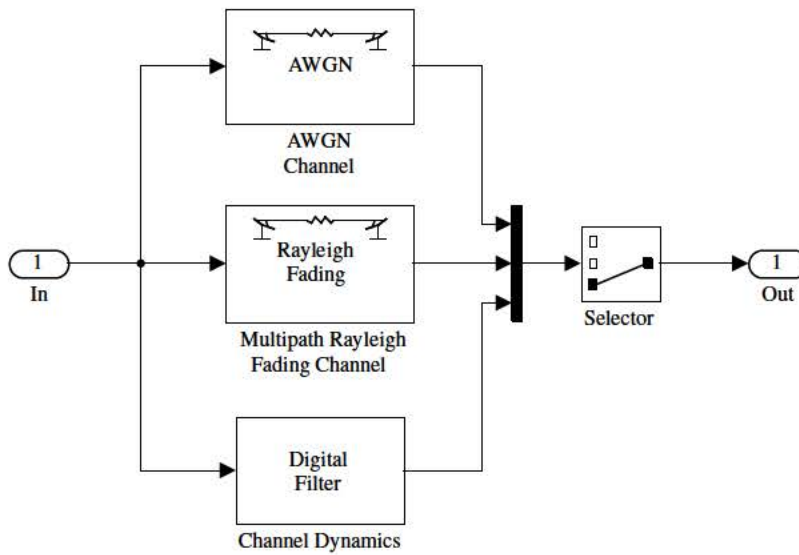
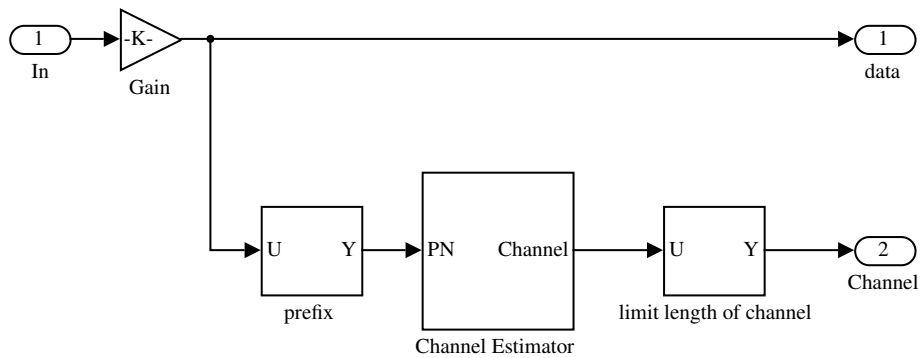
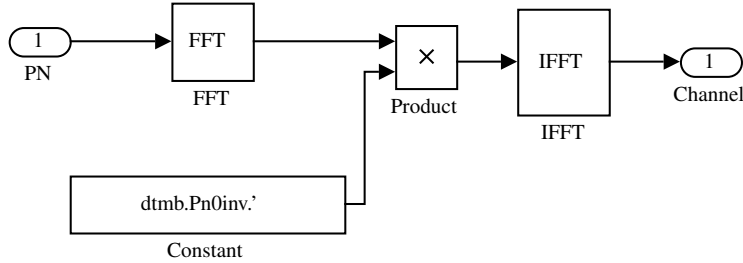


Figure A.4. Simulink model for transmission channel. It is possible to switch the type of transmission channel using the selector switch.



(a) Overall view.



(b) Channel estimator.

Figure A.6. Simulink model for the DTMB demodulator and the channel estimator within the DTMB demodulator.

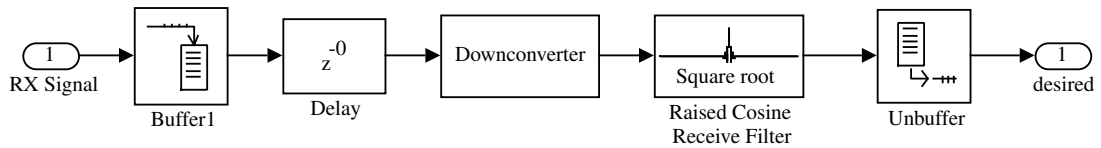


Figure A.7. Simulink model for the first communication signal demodulator.

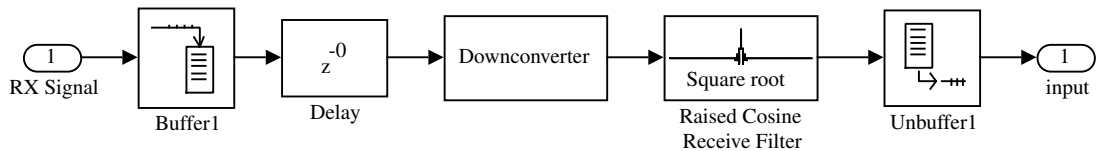


Figure A.8. Simulink model for the second communication signal demodulator.

APPENDIX B:

MATLAB Code

In this appendix, we show the MATLAB code that have been developed for this study.

B.1 Code to Run Simulation

`runsim.m` is a function that initializes the environment for the simulation, runs it and returns the results. It calls `adapt_dtmb_mqam_init.m` to initialize the parameters that do not vary between simulation runs and initialize the parameters that do vary between simulation runs.

```
function [SER_totalerr, timetaken, channelh1, simOut] = ...
    runsim(INR_dB, stopsim_maxnumsymbols, channelcoeff_error, ...
    selectfirstKcoeffs, numTrials, isSilent)
%RUNSIM Run thesis simulation.
% [SER_totalerr, timetaken, channelh1, simOut] = ...
%     runsim(INR_dB, stopsim_maxnumsymbols, channelcoeff_error, ...
%     selectfirstKcoeffs, numTrials, isSilent)
% Returns
% simOut    Contains results of simulation
% timetaken Time taken for this run
%
% Inputs
% INR_dB    Interference-to-Noise ratio, defined as comms signal over
% channel noise.
% stopsim_maxnumsymbols Run simulations for specified number of
% symbols.
% channelcoeff_error Error in estimation of channel coefficients
% E.g Specify 0.2 for a 20% error in coefficient.
% selectfirstKcoeffs The channel estimator attempts to model the
% channel as a FIR filter and outputs 255 coefficients. This
% parameter selects the first selectfirstKcoeffs coefficients to be
% used in the signal subtraction.
% numTrials Number of trials to repeat
% isSilent  If true, the Simulink model is loaded silently.
```

```

% No window will be seen. This option is used most commonly when
% doing batch runs.
%
% See also MAINPAR and SIM.

%%
filenameModel = 'adapt_dtmf_mqam';
filenameInit = strcat(filenameModel, '_init');

if isSilent
    % Load Simulink model w/o opening a window
    load_system(filenameModel)
else
    % Open Simulink model
    open_system(filenameModel)
end

%% Initialize the model variables
% Run initialization script
eval(filenameInit)
% Set the power of noise generator based on INR_dB
sigma_w = 10^( (-SIR_dB - INR_dB) / 10);
% Set the value of selectfirstKcoeffs
channel.selectfirstKcoeffs = selectfirstKcoeffs;

% if isRapid
% paramNameValStruct.SimulationMode = 'rapid';
% end

% Set options for running sim command
% See MATLAB help for more details on parameters for sim command
paramNameValStruct.ReturnWorkspaceOutputs = 'on';
paramNameValStruct.SrcWorkspace = 'current';

SER_totalerr = zeros( numTrials, 3 );
channelh1 = zeros( numTrials, length(channel.h1)*1 );

```

```

%% Run simulation

timestart = tic;
for iTrials = 1 : numTrials
    % Re-run initialization script to randomize the txn channel
    eval(filenameInit)
    simOut = sim(filenameModel, paramNameValStruct);
    SER_totalerr(iTrials, :) = simOut.get('SER_totalerr');
    channelh1(iTrials, :) = channel.h1 ;
end
timetaken = toc(timestart);

%% Compute results

% signalcomms_power = mean(abs(reshape(...
%   squeeze(simOut.get('signalcomms')),1,[])).^2);
% signaltv_power = mean(abs(reshape(...
%   squeeze(simOut.get('signaltv')),1,[])).^2);
% signalnoise_power = mean(abs(reshape(...
%   squeeze(simOut.get('signalnoise')),1,[])).^2);

% Returns SER, total errors, symbols txn
%SER_totalerr = simOut.get('SER_totalerr');

% Prints out signal-to-interference ratio (SIR) and
% interference-to-noise ratio (INR)
%fprintf('TV to Comms Ratio = %0.2f\n', ...
%   10*log10(signaltv_power/signalcomms_power) )
%fprintf('Comms to Channel Noise Ratio = %0.2f\n', ...
%   10*log10(signalcomms_power/signalnoise_power) )

% Prints out time taken
fprintf('Time taken = %0.2f min\n', timetaken/60)
% Prints out SER
%fprintf('SER = %0.2f \n', SER_totalerr(1) )

fprintf('\n')

```

end

B.2 Code for Initialization

`adapt_dtmb_mqam_init.m` is an helper function that contains the initialization parameters for the simulation. Parameters that are meant to be varied between simulation runs are initialized in `runsim.m`.

```
% ADAPT_DTMB_MQAM_INIT A helper function to put the initialization of
% parameters in a single location. It is not meant to be executed
% directly by the user.

%% DTMB code starts here

% DTMB Parameters for different cases:
dtmb.M = 16; % M-QAM
dtmb.EbN0_dB = 15; %in dB

% Rayleight Multipath CH with Doppler:
% doppler freq. in Hz (change when testing under different environment)
dtmb.fD = 80;
% Multipath time delay in (sec)
dtmb.DelayPath = [0 0.2e-6 0.5e-6 1.6e-6 2.3e-6 5e-6];
% Multipath power in (dB)
dtmb.Pwd = [-3 0 -2 -6 -8 -10];

% Frequencies
Fs = 7.56e6; % sampling and symbol rate in Hz
dtmb.NFFT = 3780; % FFT length

% compute noise variance according the specified Eb/N0
dtmb.EbN0 = 10^(dtmb.EbN0_dB /10);

% Received delay setting in error rate calculation block
dtmb.TD = zeros(1,16);
% M=16, 16-QAM
```

```

dtmb.TD(16) = 30244;
% M=4, QPSK
dtmb.TD(4) = 15122;
% M=2, BPSK
dtmb.TD(2) = 7560;

% noise variance
% signal power=unity power=OFDM data power
dtmb.Ps = 1;
% prefix length(420)
dtmb.L = dtmb.NFFT/9;
% OFDM data length(3780)
dtmb.N = dtmb.NFFT;
% prefix power boost factor
dtmb.r = 2;
dtmb.eps = eps;

% PN sequence for GI
% QPSK signal
dtmb.p0 = sign(randn(1,255)) + 1i*sign(randn(1,255));
% normalized prefix power to twice of the OFDM data part
dtmb.p0 = dtmb.p0/(sqrt(dtmb.NFFT));

dtmb.pre = dtmb.p0(255-83+1:255);
dtmb.post = dtmb.p0(1:82);
dtmb.pn = [dtmb.pre, dtmb.p0, dtmb.post];
dtmb.NGI = 255+82+83; % Length Guard Interval
dtmb.Pn0 = fft(dtmb.pn(166:dtmb.NGI));
dtmb.Pn0inv = conj(dtmb.Pn0)./(abs(dtmb.Pn0).^2 + dtmb.eps);
dtmb.zeropn = [zeros(1,dtmb.NFFT), dtmb.pn];

% bit rate
dtmb.Fb = log2(dtmb.M) * (dtmb.NFFT / (dtmb.NFFT + dtmb.NGI)) * Fs;

%% % % %
% Code added to make DTMB model work in comm signal
% This parameter is set in the runsim.m file
%sigma_w=0.01e-6; % Noise Variance

```

```

%% Dynamics of transmission channel
% with multipath
channel.PdB = [0, -10, -15];          % Power Profile in dB's
channel.tau = [0, 10/Fs, 15/Fs]; % time delays in sec
channel.n = round(channel.tau*Fs);    % time delays in samples

% convert indices from zero-based to one-based
channel.n = channel.n + 1;

channel.h0 = (randn(size(channel.PdB)) + ...
    1i*randn(size(channel.PdB))) / sqrt(2);
channel.sqrtP = 10.^(channel.PdB/20);
channel.h1 = zeros(1, max(channel.n));
channel.h1(channel.n) = channel.h0 .* channel.sqrtP;
% normalize for unit power
channel.h1 = channel.h1 / sqrt((channel.h1*channel.h1'));
channel.h1 = [0,channel.h1]; % strictly causal

% Estimated Channel
% with random error in coefficients as specified
% by channelcoeff_error
channel.h1est = channel.h1 + channelcoeff_error * channel.h1 .* ...
    ( randn(size(channel.h1)) + 1i*randn(size(channel.h1)) ) / sqrt(2);
% channel.h1est = channel.h1; % assume no errors first

% This parameter is set in the runsim.m file
% channel.selectfirstKcoeffs = 17;

%% Paramters for the Weak Comms Signal
comms.Fc = Fs/10;    % carrier frequency
comms.Fdw = comms.Fc/10; % data rate
% comms.M Number of symbols in comms signal i.e. 4-QAM or 16-QAM.
comms.M = 4; % 4-QAM comms signal

%% % % %

```

```

% Signal to Interference Ratio (SIR)
% defined as TV signal / comms signal
SIR_dB = 30;

% LMS weights vector
%n = 0:length(dtmf.DelayPath)-1;
LMSfilter.length = 50;
LMSfilter.weights = zeros(1,LMSfilter.length);
LMSfilter.mu = 0.0001;    % stepsize of LMS

% Number of data points to keep for debug
keepLastMpoints = 1;

% % % %

```

B.3 Code to Enable Parallel Computing

mainpar.m is a script that distributes the running of stimulation runs across multiple processors, allowing parallelization to take place.

```

% MAINPAR Main job to start other tasks for parallerization.
% This is the main file to run to generate a complete
% SER-INR curve. To determine the SER for a single INR value,
% see RUNSIM.
%
% The following internal variables within the script file
% control the parameters of the simulation.
%
% INR_dB is an array that sets the INRs to run for.
% stopsim_maxsym sets the number of symbols transmitted
% for that particular value of INR before stopping the
% simulation.
% num_Trials is the number of trials to repeat.
% selectfirstKcoeffs sets the number of coefficients to keep
% in the estimated channel impulse response.
% channelcoeff_error sets the percentage error in the channel
% coefficient values.

```

```

%
% Note that the Simulink model, adapt_dtmb_mqam.slx, determines
% whether the simulation is using selectfirstKcoeffs or
% channelcoeff_error.
%
% See also RUNSIM, PARFOR and MATLABPOOL.

%clearvars
%close all

%% Set parameters here
INR_dB = (-5 : 5 : 50)';

% start with small number to test parfor
stopsim_maxsym = 4.2e3 * 10 * ones(size(INR_dB));

% Adjust channelcoeff_error or selectfirstKcoeff depending on test case
% Remember to adjust the Simulink model and the filename to save the
% results to as well
channelcoeff_error = 0.3;
selectfirstKcoeffs = 17;
numTrials = 100;

% length of channelh1. Depends on Fs and channel parameters
% this is used to do preallocation
channeltxn_len = 17;

%% Loop thru simulations

elapsed = zeros(size(INR_dB));
SER = zeros( numTrials, 3, size(INR_dB, 1) );
channelcoeffs = zeros( numTrials, channeltxn_len*1, size(INR_dB, 1) );
parfor i = 1 : length(INR_dB)
    %[SER(i,:), elapsed(i), ~] = runsim(INR_dB(i), stopsim_maxsym(i), ...
    % comms_M, selectfirstKcoeffs, numTrials, true);
    [SER(:, :, i), elapsed(i), channelcoeffs(:, :, i), ~] = ...
        runsim(INR_dB(i), stopsim_maxsym(i), ...
            channelcoeff_error, selectfirstKcoeffs, numTrials, true);

```

```

end

%% Tabulate results

%results = [INR_dB SER];
results = [ ...
    reshape( repmat(INR_dB,1,numTrials)', [numTrials*length(INR_dB), 1]), ...
    reshape( permute(SER,[1 3 2]) , [numTrials*length(INR_dB) 3] )
];

channeltxn = reshape( permute(channelcoeffs,[1 3 2]) , ...
    [ numTrials*length(INR_dB), channeltxn_len] );

% Save handle of figure
hdl = zeros(1,2);
hdl(1) = figure;
plot(results(:,1), results(:,2) )
xlabel('INR (dB)')
ylabel( sprintf( 'SER over %d trials', numTrials) )
title( sprintf('selectfirstKcoeffs = %d channelcoefferror = %.2f', ...
    selectfirstKcoeffs, channelcoeff_error) )

results_cumu = [ INR_dB, zeros( length(INR_dB), 4)];
for i = 1:length(INR_dB),
    % Sum of error encountered and symbols transmitted
    results_cumu(i, 4:5) = ...
        sum( results( numTrials*(i-1)+1:numTrials*i, 3:4 ) );
    % Mean SER
    results_cumu(i, 2) = ...
        mean( results( numTrials*(i-1)+1:numTrials*i, 2 ) );
    % Median SER
    results_cumu(i, 3) = ...
        median( results( numTrials*(i-1)+1:numTrials*i, 2 ) );
end

hdl(2) = figure;
plot(results_cumu(:,1), results_cumu(:,2), ...
    results_cumu(:,1), results_cumu(:,3) )

```

```

xlabel('INR (dB)')
ylabel( sprintf( 'SER over %d trials', numTrials) )
title( sprintf( strcat('Cumulative. selectfirstKcoeffs = ', ...
    '%d channelcoefferror = %.2f'), ...
    selectfirstKcoeffs, channelcoeff_error) )
legend('Mean', 'Median')

hdl(3) = figure;
semilogy(results_cumu(:,1), results_cumu(:,2), ...
    results_cumu(:,1), results_cumu(:,3) )
xlabel('INR (dB)')
ylabel( sprintf( 'SER over %d trials', numTrials) )
title( sprintf( strcat( 'Cumulative. selectfirstKcoeffs = ', ...
    '%d channelcoefferror = %.2f'), ...
    selectfirstKcoeffs, channelcoeff_error) )
legend('Mean', 'Median')

%% Save results
filename_results = ...
    sprintf( strcat('Results/results_%s_NLMS_selectfirstKcoeff%d_', ...
        '%dtrials_%dsymbols'), ...
        datestr(now, 'yyyymmdd'), selectfirstKcoeffs, numTrials, ...
        stopsim_maxsym(1) );
save_results(filename_results, ...
    hdl, results, results_cumu, channeltxn, ...
    numTrials, selectfirstKcoeffs, channelcoeff_error);

%% Clean up variables
%clear INR_dB stopsim_maxsym selectfirstKcoeffs numTrials i ...
% channelcoeff_error channelcoeffs channeltxn_len SER
clear INR_dB stopsim_maxsym i channelcoeffs channeltxn_len SER hdl
fprintf('All done!\n')

function save_results(filename_main, handle, results, ...
    results_cumu, channeltxn, numTrials, selectfirstKcoeffs, ...
    channelcoeff_error )
% SAVE_RESULTS Saves the results of a completed simulation run
%
```

```

% save_results(filename_main, handle, results, ...
%     results_cumu, channeltxn, numTrials, selectfirstKcoeffs, ...
%     channelcoeff_error )
%
% This function should not be called directly by the user under
% normal situations. Designed to be a helper function to MAINPAR.
%
% See also MAINPAR.

% Saves the variables
save(filename_main, 'results', 'results_cumu', 'channeltxn', ...
      'numTrials', 'selectfirstKcoeffs', 'channelcoeff_error' )

% saves Figure 1, 2 and 3
% Intentionally not use 'i' as loop counter to avoid clash
for iCount = 1:3
    filename = strcat( filename_main, sprintf( '-%d', iCount ) );
    saveas(handle(iCount), filename, 'fig')
end

% Clean up variables
clear filename_main filename iCount
end

```

THIS PAGE INTENTIONALLY LEFT BLANK

APPENDIX C: Supplementary Plots

In this appendix, we present additional plots to supplement the information provided in Chapter 4.

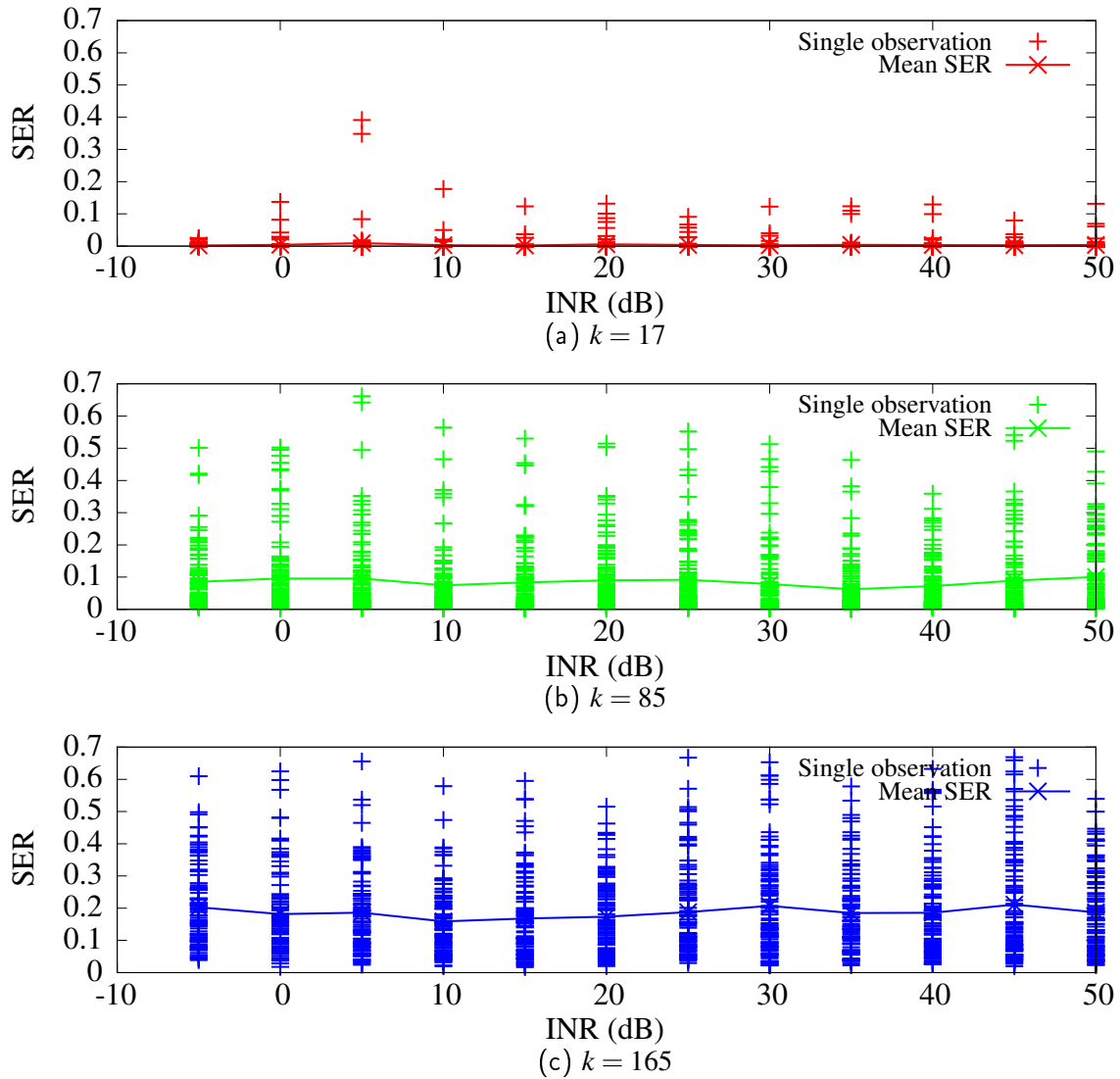


Figure C.1. Plot showing distribution of the 100 observations of SER for each INR value for different number of coefficients k in $\hat{h}(n)$. The y-axis range is kept constant throughout for comparison.

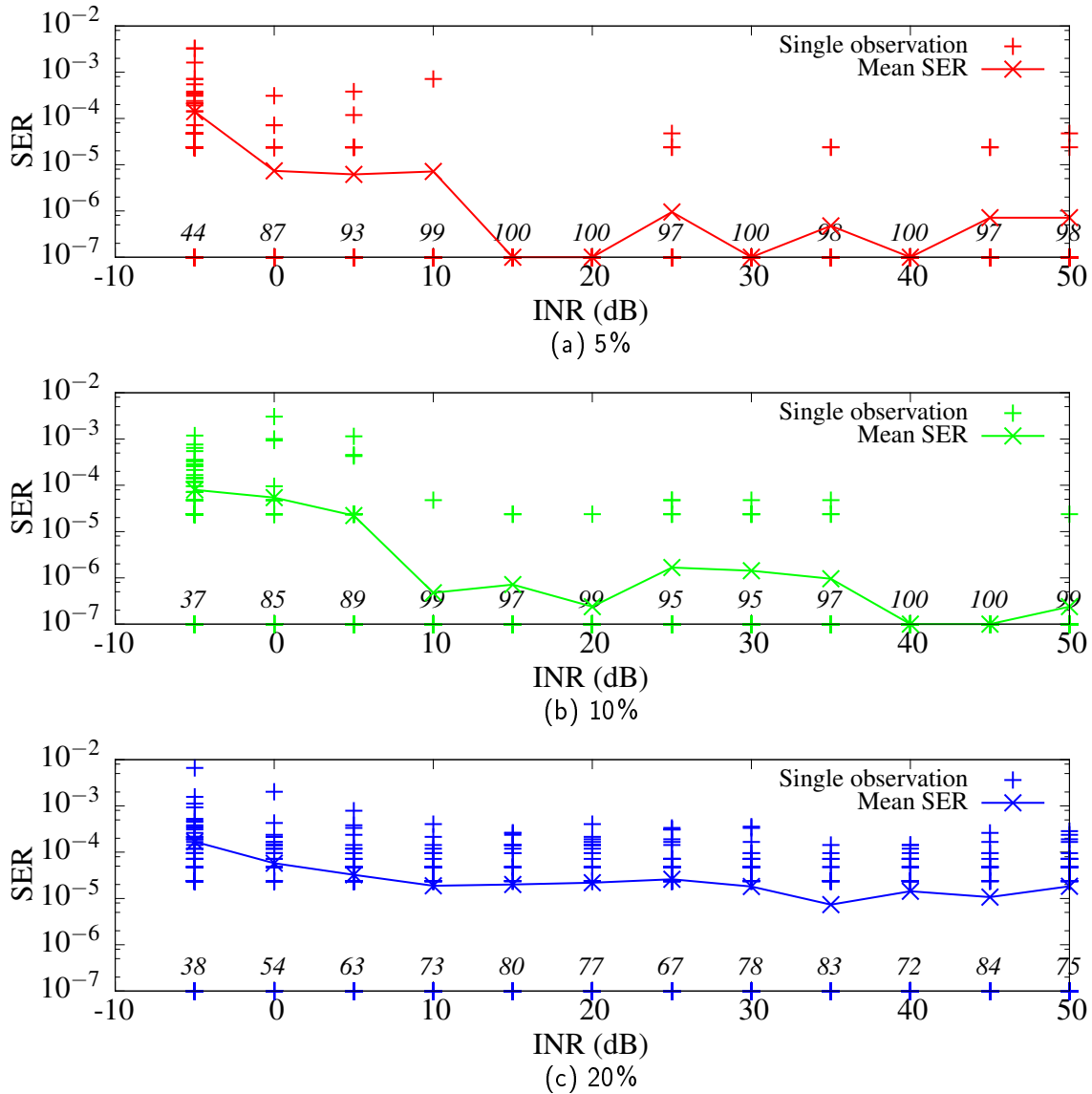


Figure C.2. Plot showing distribution of the 100 observations of SER for each INR value for different percentages of error in the channel coefficients. The y-axis range is kept constant throughout for comparison. SER values equal to zero are represented as 10^{-7} on the logarithmic axis. The numbers in italics just above the x-axis denote the number of SER values that are equal to zero.

List of References

- [1] R. Gooch and B. Sublett, "Demodulation of cochannel QAM signals," in *Proc. IEEE Int. Conf. Acoust., Speech, Signal Process. (ICASSP)*, vol. 2, Glasgow, UK, May 1989, pp. 1392–1395.
- [2] P. Ranta, A. Hottinen, and Z.-C. Honkasalo, "Co-channel interference cancelling receiver for TDMA mobile systems," in *Proc. IEEE 1995 Int. Conf. Commun.*, vol. 1, Seattle, WA, June 1995, pp. 17–21.
- [3] K. Giridhar, S. Chari, J. Shynk, R. Gooch, and D. Artman, "Joint estimation algorithms for cochannel signal demodulation," in *1993 IEEE Int. Conf. Commun.*, vol. 3, Geneva, Switzerland, May 1993, pp. 1497–1501.
- [4] M. Osato, H. Kobashi, R. Omaki, T. Hara, and M. Okada, "Development of signal canceller in the carrier super-positioning satellite networks," in *Proc. 3rd Int. Conf. Wireless and Mobile Commun. (ICWMC '07)*, Guadeloupe, Mar. 2007, pp. 35–35.
- [5] M. Ichikawa, T. Hara, M. Okada, H. Yamamoto, and K. Ando, "Fast and accurate canceller on carrier super-positioning for VSAT frequency re-use," in *Proc. IEEE Wireless Commun. and Netw. Conf.*, vol. 3, Mar. 2005, pp. 1479–1484.
- [6] M. Dankberg, "Paired carrier multiple access (PCMA) for satellite communications," in *17th AIAA Int. Commun. Satellite Syst. Conf. and Exhibit*, vol. 3, Yokohama, Japan, Feb. 1998, pp. 1479–1484.
- [7] R. Cristi, M. P. Fargues, and M. E. Hagstette, "Detection of a weak communication signal in the presence of a strong co-channel TV broadcast interferer," Oct. 2013, unpublished.
- [8] M. E. Hagstette, "Extraction of a weak co-channel interfering communication signal using complex independent component analysis," M.S. thesis, Dept. Elect. and Comput. Eng., Naval Postgraduate School, Monterey, CA, June 2013.
- [9] M. E. Hagstette, M. P. Fargues, and R. Cristi, "Extraction of a weak co-channel interfering communication signal using complex independent component analysis," in *Conf. Rec. 47th Asilomar Conf. Signals, Syst. and Comput.*, Pacific Grove, CA, Nov. 2013, pp. 1171–1175.
- [10] A. Sajid, "Detection of a low power communication signal in the presence of a strong co-channel TV broadcast interference using Kalman filter," M.S. thesis, Dept. Elect. and Comput. Eng., Naval Postgraduate School, Monterey, CA, Dec. 2014.

- [11] H.-C. Lai, “Simulink-based implementation and performance analysis of TDS-OFDM in time-varying environments,” M.S. thesis, Dept. Elect. and Comput. Eng., Naval Postgraduate School, Monterey, CA, Sep. 2014.
- [12] *Framing Structure, Channel Coding and Modulation for Digital Television Terrestrial Broadcasting System, Chinese National Standard*, Standardization Administration of the People’s Republic of China GB 20 600-2006, Sep. 2006.
- [13] J. Song, Z. Yang, L. Yang, K. Gong, C. Pan, J. Wang, and Y. Wu, “Technical review on Chinese digital terrestrial television broadcasting standard and measurements on some working modes,” *IEEE Trans. Broadcast.*, vol. 53, no. 1, pp. 1–7, Mar. 2007.
- [14] R. Karamchedu. (2009, May 4). Does China have the best digital television standard on the planet? [Online]. Available: <http://spectrum.ieee.org/consumer-electronics/standards/does-china-have-the-best-digital-television-standard-on-the-planet/0>
- [15] The DVB Project. (2014, Dec. 8). DVB-T2 map. [Online]. Available: https://www.dvb.org/resources/public/images/site/dvb-t_map.pdf
- [16] B. Widrow, J. R. Glover, Jr., J. M. McCool, J. Kaunitz, C. S. Williams, R. H. Hearn, J. R. Zeidler, E. Dong, Jr., and R. C. Goodlin, “Adaptive noise cancelling: Principles and applications,” in *Proc. IEEE*, vol. 63, no. 12, Dec. 1975, pp. 1692–1716.
- [17] J. R. Glover Jr., “Adaptive noise canceling applied to sinusoidal interferences,” *IEEE Trans. Acoust., Speech, Signal Process.*, vol. 25, no. 6, pp. 484–491, Dec. 1977.
- [18] D. G. Manolakis, V. K. Ingle, and S. M. Kogon, *Statistical and Adaptive Signal Processing : Spectral Estimation, Signal Modeling, Adaptive Filtering, and Array Processing*. Boston: Artech House, 2005.
- [19] W. Zhang, Y. Guan, W. Liang, D. He, F. Ju, and J. Sun, “An introduction of the Chinese DTTB standard and analysis of the PN595 working modes,” *IEEE Trans. Broadcast.*, vol. 53, no. 1, pp. 8–13, Mar. 2007.
- [20] F. Yang, J. Wang, J. Wang, J. Song, and Z. Yang, “Novel channel estimation method based on PN sequence reconstruction for Chinese DTTB system,” *IEEE Trans. Consum. Electron.*, vol. 54, no. 4, pp. 1583–1589, Nov. 2008.
- [21] W. Zhang, Y. Guan, W. Liang, and M. Wang, “Joint channel estimation and equalization algorithm for DTMB receivers,” in *IEEE Int. Symp. Broadband Multimedia Syst. and Broadcast. (BMSB)*, June 2013, pp. 1–5.
- [22] MathWorks, Natick, MA. (2014, Oct.). *Simulink 2014b Documentation*. [Online]. Available: <http://www.mathworks.com/help/simulink/gui/solver-pane.html#bq994cq-1>

- [23] T. Claasen and W. Mecklenbrauker, "Adaptive techniques for signal processing in communications," *IEEE Commun. Mag.*, vol. 23, no. 11, pp. 8–19, Nov. 1985.
- [24] J. G. Proakis, *Digital Communications*. Boston: McGraw-Hill, 2001.
- [25] M. Ozdemir and H. Arslan, "Channel estimation for wireless OFDM systems," *IEEE Commun. Surveys Tuts.*, vol. 9, no. 2, pp. 18–48, 2nd Quarter 2007.

THIS PAGE INTENTIONALLY LEFT BLANK

Initial Distribution List

1. Defense Technical Information Center
Ft. Belvoir, Virginia
2. Dudley Knox Library
Naval Postgraduate School
Monterey, California